Environment International 178 (2023) 108081

Contents lists available at ScienceDirect

Environment International

journal homepage: www.elsevier.com/locate/envint

Full length article

The variability of mass concentrations and source apportionment analysis of equivalent black carbon across urban Europe

Marjan Savadkoohi [a,b,*], Marco Pandolfi [a,*], Cristina Reche [a], Jarkko V. Niemi [c], Dennis Mooibroek [d], Gloria Titos [e], David C. Green [f,g], Anja H. Tremper [f], Christoph Hueglin [h], Eleni Liakakou [i], Nikos Mihalopoulos [i], Iasonas Stavroulas [i], Begoña Artiñano [j], Esther Coz [j], Lucas Alados-Arboledas [e], David Beddows [k], Véronique Riffault [l], Joel F. De Brito [l], Susanne Bastian [m], Alexia Baudic [n], Cristina Colombi [o], Francesca Costabile [p], Benjamin Chazeau [q,r], Nicolas Marchand [q], José Luis Gómez-Amo [s], Víctor Estellés [s], Violeta Matos [s], Ed van der Gaag [t], Grégory Gille [u], Krista Luoma [v], Hanna E. Manninen [c], Michael Norman [w], Sanna Silvergren [w], Jean-Eudes Petit [x], Jean-Philippe Putaud [y], Oliver V. Rattigan [z], Hilkka Timonen [aa], Thomas Tuch [ab], Maik Merkel [ab], Kay Weinhold [ab], Stergios Vratolis [ac], Jeni Vasilescu [ad], Olivier Favez [ae], Roy M. Harrison [k,af], Paolo Laj [ag,ah], Alfred Wiedensohler [ab], Philip K. Hopke [ai], Tuukka Petäjä [ah], Andrés Alastuey [a], Xavier Querol [a]

[a] Institute of Environmental Assessment and Water Research (IDAEA-CSIC), Barcelona, Spain
[b] Department of Mining, Industrial and ICT Engineering (EMIT), Manresa School of Engineering (EPSEM), Universitat Politècnica de Catalunya (UPC), 08242, Manresa, Spain
[c] Helsinki Region Environmental Services Authority (HSY), Helsinki, Finland
[d] Centre for Environmental Monitoring, National Institute for Public Health and the Environment (RIVM), the Netherlands
[e] Andalusian Institute for Earth System Research (IISTA-CEAMA), University of Granada, Granada, Spain
[f] MRC Centre for Environment and Health, Environmental Research Group, Imperial College London, UK
[g] NIHR HPRU in Environmental Exposures and Health, Imperial College London, UK
[h] Laboratory for Air Pollution and Environmental Technology, Swiss Federal Laboratories for Materials Science and Technology (Empa), Duebendorf, Switzerland
[i] Institute for Environmental Research & Sustainable Development, National Observatory of Athens, Athens, Greece
[j] Centro de Investigaciones Energéticas, Medioambientales y Tecnológicas, Department of Environment, CIEMAT, Madrid, Spain
[k] Division of Environmental Health & Risk Management, School of Geography, Earth & Environmental Sciences, University of Birmingham, Edgbaston, Birmingham, UK
[l] IMT Nord Europe, Institut Mines-Télécom, Univ. Lille, Centre for Energy and Environment, Lille, France
[m] Saxon State Office for Environment, Agriculture and Geology/Saxon State Department for Agricultural and Environmental Operations, Dresden, Germany
[n] AIRPARIF (Ile de France Air Quality Monitoring network), Paris, France
[o] Arpa Lombardia, Settore Monitoraggi Ambientali, Unità Operativa Qualità dell'Aria, Milano, Italy
[p] Institute of Atmospheric Sciences and Climate-National Research Council, Rome, Italy
[q] Aix Marseille Univ., CNRS, LCE, Marseille, France
[r] Laboratory of Atmospheric Chemistry, Paul Scherrer Institute, 5232 Villigen, Switzerland
[s] Solar Radiation Group. Dept. Earth Physics and Thermodynamics, University of Valencia, Burjassot, Spain
[t] DCMR Environmental Protection Agency, Department Air and Energy, Rotterdam, the Netherlands
[u] AtmoSud, Regional Network for Air Quality Monitoring of Provence-Alpes-Cote-d'Azur, Marseille, France
[v] Institute for Atmospheric and Earth System Research/Physics, Faculty of Science, University of Helsinki, Helsinki, Finland
[w] Environment and Health Administration, SLB-analysis, Stockholm, Sweden
[x] Laboratoire des Sciences du Climat et de l'Environnement, CEA/Orme des Merisiers, Gif-sur-Yvette, France
[y] European Commission, Joint Research Centre (JRC), Ispra, Italy
[z] Division of Air Resources, New York State Dept of Environmental Conservation, NY, USA
[aa] Atmospheric Composition Research, Finnish Meteorological Institute, Helsinki, Finland
[ab] Leibniz Institute for Tropospheric Research (TROPOS), Leipzig, Germany
[ac] Environmental Radioactivity Laboratory, Institute of Nuclear & Radiological Sciences & Technology, Energy & Safety, N.C.S.R. "Demokritos", Athens, Greece
[ad] National Institute of Research and Development for Optoelectronics INOE 2000, Magurele, Romania
[ae] Institut National de l'Environnement Industriel et des Risques (INERIS), Verneuil-en-Halatte, France
[af] Department of Environmental Sciences, Faculty of Meteorology, Environment and Arid Land Agriculture, King Abdulaziz University, Jeddah, Saudi Arabia
[ag] Univ. Grenoble, CNRS, IRD, IGE, 38000 Grenoble, France

* Corresponding authors.
E-mail addresses: marjan.savadkoohi@idaea.csic.es (M. Savadkoohi), marco.pandolfi@idaea.csic.es (M. Pandolfi).

https://doi.org/10.1016/j.envint.2023.108081
Received 14 March 2023; Received in revised form 29 June 2023; Accepted 30 June 2023
Available online 5 July 2023

[ah] Institute for Atmospheric and Earth System Research/Physics (INAR), Faculty of Science, University of Helsinki, Helsinki, Finland
[ai] Department of Public Health Sciences, University of Rochester School of Medicine & Dentistry, Rochester, NY, USA

ARTICLE INFO

Handling Editor: Olga Kalantzi

Keywords:
Air quality
European urban environment
Filter absorption photometer
Source apportionment
eBC

ABSTRACT

This study analyzed the variability of equivalent black carbon (eBC) mass concentrations and their sources in urban Europe to provide insights into the use of eBC as an advanced air quality (AQ) parameter for AQ standards. This study compiled eBC mass concentration datasets covering the period between 2006 and 2022 from 50 measurement stations, including 23 urban background (UB), 18 traffic (TR), 7 suburban (SUB), and 2 regional background (RB) sites. The results highlighted the need for the harmonization of eBC measurements to allow for direct comparisons between eBC mass concentrations measured across urban Europe. The eBC mass concentrations exhibited a decreasing trend as follows: TR > UB > SUB > RB. Furthermore, a clear decreasing trend in eBC concentrations was observed in the UB sites moving from Southern to Northern Europe. The eBC mass concentrations exhibited significant spatiotemporal heterogeneity, including marked differences in eBC mass concentration and variable contributions of pollution sources to bulk eBC between different cities. Seasonal patterns in eBC concentrations were also evident, with higher winter concentrations observed in a large proportion of cities, especially at UB and SUB sites. The contribution of eBC from fossil fuel combustion, mostly traffic (eBC_T) was higher than that of residential and commercial sources (eBC_{RC}) in all European sites studied. Nevertheless, eBC_{RC} still had a substantial contribution to total eBC mass concentrations at a majority of the sites. eBC trend analysis revealed decreasing trends for eBC_T over the last decade, while eBC_{RC} remained relatively constant or even increased slightly in some cities.

1. Introduction

Black carbon (BC) is a primary particulate pollutant generated by combustion processes (Bond et al., 2013); it is one of the key components of ambient particulate matter (PM). BC emissions originate from several anthropogenic combustion sources, such as the diesel engines of on-road and off-road vehicles (i.e., transportation and industry), maritime shipping (Geels et al., 2021; Lack and Corbett, 2012; Zhang et al., 2019a; Zhang et al., 2019b), domestic solid fuel (biomass-burning and coal combustion), and other combustion processes (e.g., residential heating) (Bond et al., 2013; Briggs and Long, 2016; Intergovernmental Panel on Climate Change [IPCC], 2021).

BC terminology is diverse and there are many uncertainties associated with the definitions and methods used to measure BC (Petzold et al., 2013; Grange et al., 2020). Several previous studies have proposed varying definitions and recommended standard terminology for carbonaceous aerosols, and the nomenclature used for BC can be confusing (Bond et al., 2013; Petzold et al., 2013). Equivalent BC (eBC) is commonly defined as the mass concentration of BC as indirectly determined by light absorption techniques such as filter-based absorption photometers (Petzold et al., 2013). Filter-based absorption photometers measure the attenuation (σ_{ATN}) or transmission of light through a particle-loaded filter tape and convert them to the absorption of light. These optical instruments, such as the aethalometer (AE) and the multi-angle absorption photometer (MAAP), have been widely used to estimate eBC mass concentrations from the amount of light absorbed by the particles collected on filter tape samples using a conversion factor known as a mass absorption cross-section (MAC). These techniques thus indirectly determine the eBC mass concentration based on particle light absorption coefficient measurements at specific wavelengths. Thus, eBC is defined operationally by the method used for its measurements (Moosmüller et al., 2009; Petzold et al., 2013). Consequently, the term eBC will be used throughout this study as all eBC data were calculated using filter-absorption photometers and their respective instrument software.

Unlike most components of atmospheric aerosol that have a climate cooling effect, eBC exhibits a substantial positive radiative forcing (warming) effect due to its strong light-absorption, albeit with significant quantitative uncertainties (Bond et al., 2013; IPCC, 2021; Ivančič et al., 2022; Lack and Cappa, 2010). There are no generally agreed standards on eBC measurement methods and their related uncertainties (Petzold et al., 2013). Previous intercomparisons of aerosol absorption photometers have shown that there is a significant variation in the light-absorption response of aerosol particles on different instruments due to source contributions, sample flow, and spot size (Cuesta-Mosquera et al., 2021; Müller et al., 2011). The Aerosol, Clouds and Trace Gases Research Infrastructure (ACTRIS) (Measurement guidelines, 2022) and Working Group WG 35 of the European Committee for Standardization (CEN) have attempted to provide recommendations in order to harmonize eBC measurements. However, the need for a broad implementation of these recommendations is evident from the wide array of protocols used to measure eBC across Europe.

eBC-related research in urban areas attracted a significant amount of attention due to the potential health impacts of soot (i.e., combustion particles made of a core of eBC and coating of organic and sulfur compounds) of which eBC is a tracer (Kumar et al., 2020; Segersson et al., 2017). The adverse impacts of eBC on public health and climate—at both local and global scales—have been extensively documented (Briggs and Long, 2016; World Health Organization [WHO], 2021). Nevertheless, available data on eBC and associated health effects have not been sufficient to provide consistent results to set up or discard air quality (AQ) guidelines (WHO, 2021). Furthermore, eBC itself does not necessarily have a negative impact on public health; rather, it is the presence of other species condensed onto eBC particles that may cause health issues (WHO, 2012). Nevertheless, it has been concluded that eBC is a better indicator of harmful particulate substances from combustion sources (especially traffic) than the mass of undifferentiated atmospheric PM. Thus, the closer monitoring of eBC may improve the assessment of policy actions to abate air pollution from combustion sources while also providing more consistent data for epidemiological analysis (Geng et al., 2013; WHO, 2012, 2021).

Several studies have investigated the variability of eBC mass concentrations in specific urban, traffic, and regional background environments. Some of these also focused on the source apportionment (SA) of eBC, such as the proportion of eBC that stems from the burning of fossil fuels in vehicular exhaust emissions (road traffic; eBC_T) and solid fuel combustion (mainly from residential and commercial wood and coal burning; eBC_{RC}) (Blanco-Donado et al., 2022; Grange et al., 2020; Helin et al., 2018; Liakakou et al., 2020; Mbengue et al., 2020; Milinković et al., 2021; Minderytė et al., 2022; Mousavi et al., 2018, 2019, Sandradewi et al., 2008a,b). These studies have been individually reported on the climatology, characterization, and variability of eBC in different regions (Crilley et al., 2015; Favez et al., 2009; Grange et al., 2020; Helin et al., 2018; Jafar and Harrison, 2021; Krecl et al., 2011;

Kutzner et al., 2018; Laborde et al., 2013; Luoma et al., 2021; Lyamani et al., 2011; Mousavi et al., 2019; Pandolfi et al., 2014; Schaap and Denier van der Gon, 2007; Singh et al., 2018; Titos et al., 2017; Vanderstraeten et al., 2011). However, to the best of our knowledge, a large-scale database that allows for access to eBC data across urban Europe has not been implemented.

The Research Infrastructures Services Reinforcing Air Quality Monitoring Capacities in EU Urban & Industrial AreaS (RI-URBANS) project is a European H2020-Green Deal initiative that aims to provide tools for the measurement and analysis of advanced AQ parameters (RI-URBANS, 2020), including eBC, ultrafine particles, and oxidative potential in urban environments, which will consequently allow for the enhanced assessment of AQ policies. Thus, it is necessary to harmonize measurement, instrumentation, and data analysis protocols to provide comparable data from different cities across Europe.

One of the objectives of RI-URBANS is to evaluate the application of advanced AQ metrics, such as eBC, in urban environments and other air pollution hotspots. In line with this objective, this study aims to 1) compile and interpret long-term ambient eBC measurements across urban Europe; 2) analyze the current measurement corrections, concentration levels, and spatial and temporal variability covering a wide variety of climate and urban patterns; and 3) quantify the contribution of eBC_T and eBC_{RC} to bulk urban eBC mass concentrations. This long-term eBC observations provide valuable information that can be used to evaluate its potential to improve policy assessments as an AQ standard as well as better protect human health (Irwin et al., 2015; Janssen et al., 2011; WHO, 2012). The harmonized urban eBC data compiled in this study will be used in epidemiological evaluations, for model validation, and for improving emission inventories in future investigations.

2. Methodology

2.1. Measurement sites

This study aimed to evaluate the long-term phenomenology of eBC by compiling datasets on eBC mass concentrations from 50 European monitoring sites, covering various periods between 2006 and 2022. These 50 measurement sites include 23 urban background (UB) sites, 18 traffic (TR) sites, 7 sub-urban background (SUB) sites, and 2 regional background (RB) sites across 29 cities in 11 European countries. These categories were selected based on the descriptions used for the classification of AQ monitoring sites (European Environmental Agency [EEA],

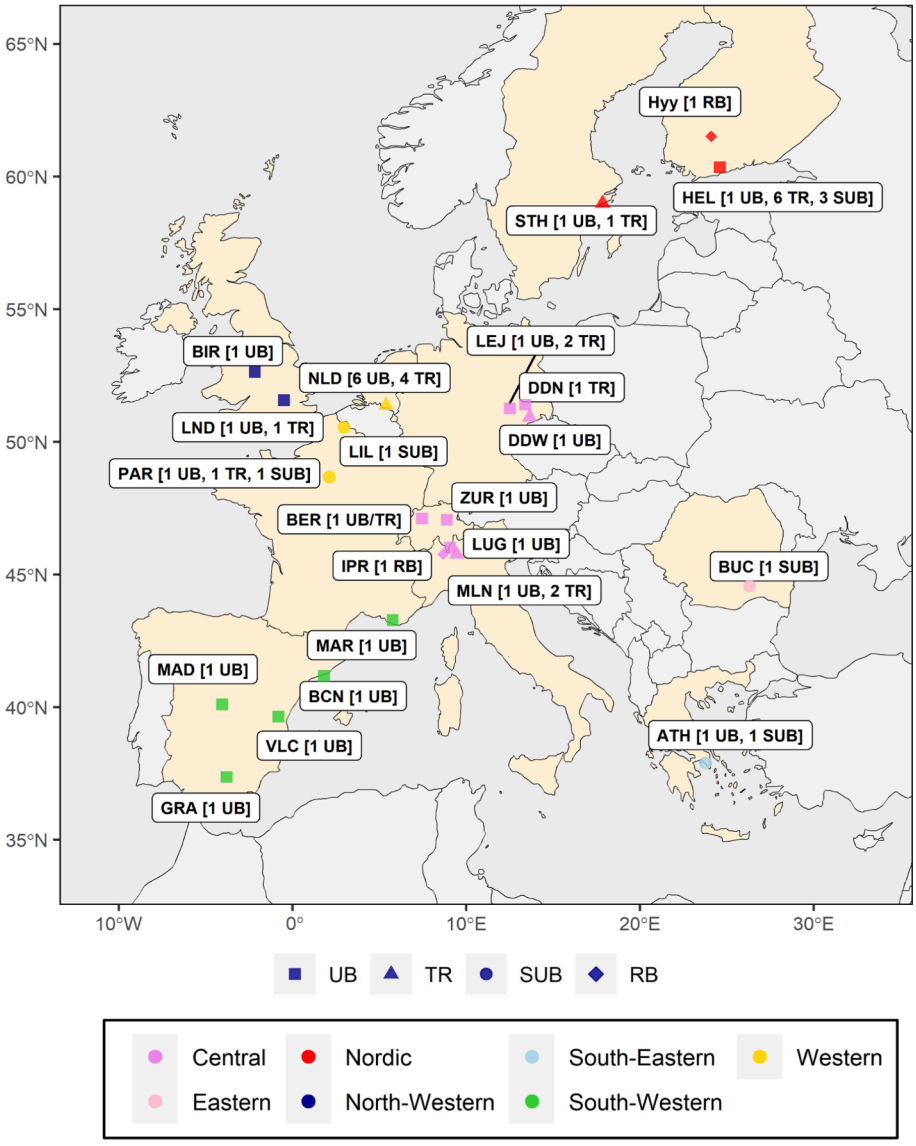

Fig. 1. The location and type of monitoring sites that have supplied eBC data to this study. UB: urban background; SUB: suburban background; TR: traffic; RB: regional background. The colors correspond to the seven main geographic regions around Europe.

2023; UK AIR, 2023). As this study focuses on European urban environments, a few suburban and regional background sites were selected to ensure better spatial coverage and a greater understanding of eBC variability. However, it should be noted that their eBC trends cannot be considered to be representative of the variability for all European RB sites, as previously reported by Laj et al. (2020) or Collaud Coen et al. (2020). Fig. 1 describes the distribution of monitoring sites that are currently providing measurements of eBC mass concentrations. The measurement sites were grouped into seven categories based on their geographical location (Northern, Eastern, Western, Central, South-Eastern, South-Western, and North-Western); this categorization scheme follows from the grouping of sites in previous European phenomenology studies (Pandolfi et al., 2018; Putaud et al., 2010). The highlighted areas in Fig. 1 are indicative of geographical classifications.

The data coverage mainly comprises UB and TR sites, located in cities from different climate zones of Europe that are affected by different road traffic volumes, industrial sources, power plant emissions, harbors, domestic sources, etc. As shown in Fig. 1, the spatial coverage over Europe is not homogeneous: there is a higher density of measurement sites over central Europe and a much lower density of sites in Eastern Europe—this is denoted by the grey area in which eBC measurements were not available.

2.2. Instrumentation

Table S1 summarizes the instruments used to measure eBC mass concentrations in the 50 sites. In addition to differences in instrumentation, relevant distinct measurement settings have also been noted (e.g., different sampling inlet heights). eBC mass concentrations were primarily monitored by filter-based absorption photometers. eBC data were obtained through the use of MAAPs (Thermo Scientific, discontinued) or aethalometers (mainly AE33 model; Magee Scientific). The recommended terminology and measurement techniques for these instruments have been comprehensively discussed in Petzold and Schönlinner (2004), Petzold et al. (2005), and Drinovec et al. (2015).

The MAAP was developed to decrease the uncertainties in absorption measurements (b_{abs}). It measures the transmitted, backscattered light through the aerosol-loaded filter tape and then applies a radiative transfer scheme to convert the measurements into particle light absorption coefficients. It determines the particle light absorption coefficient using a 670 nm operating wavelength (as specified by the manufacturer), while its actual wavelength is 637 nm (Müller et al., 2011). The default MAC setting of 6.6 $m^2\ g^{-1}$ and a nominal wavelength of 670 nm are used to convert the optically measured absorption data to eBC mass concentrations. The instrument also accounts for filter-loading-related artifacts that can affect the calculation of the absorption coefficient (Petzold and Schönlinner, 2004). However, given the discontinued production of the MAAP, its future availability for long-term observations is uncertain. Furthermore, MAAP data were not accessible from all 50 monitoring sites investigated in this study, as some sites deployed other types of absorption photometers, as discussed in the following section.

The AE33 dual-spot Aethalometer (Magee Scientific) measures the attenuation of light (σ_{ATN}) through an aerosol-loaded filter tape samples and provides particle light absorption coefficients at seven different wavelengths (370, 470, 520, 590, 660, 880, and 950 nm). It converts the optical absorbance into eBC mass concentrations using a default MAC value of 7.77 $m^2\ g^{-1}$ at 880 nm. AE33 has been equipped with a real-time filter loading effect compensation algorithm based on the dual-spot measurements (Drinovec et al., 2015). Older Aethalometer models such as the AE31 and AE22 measure light attenuation through the filter at seven (AE31) and two (AE22; 370 and 880 nm) wavelengths using an instrument-derived mass attenuation cross section value of 16.62 $m^2\ g^{-1}$ at 880 nm. However, these models require correction for loading effects, and algorithms for correcting this artifact have been developed and tested by different researchers (Collaud Coen et al., 2020; Virkkula, 2021; Virkkula et al., 2007; Weingartner et al., 2003).

In brief, of the 50 observation sites present across Europe, the MAAP was the most commonly used instrument for measuring eBC mass concentrations, used at 30 of the 50 sites. The MAAP was primarily used in measurement sites across Western and Northern Europe (see Table S1). Both a MAAP and an aethalometer were deployed in parallel at a few sites (BCN, GRA, STH, MLN, and SMR). In the RI-URBANS database, data from 23 sites were obtained using the AE33 instrument, while only a few stations provided data from AE22 and AE31 instruments (e.g., LND, SMR, and VLC). Table S1 also provides information about the geographic region, site, city, country, station type, coordinates, altitude, measurement height, data coverage, and type of data received (more details can be found in Section 2.3).

2.3. Data treatment and pre-processing

This study required the use of station metadata, including station information (e.g., type, altitude, height, and coordinates), the filter absorption photometer used, the measurement method, and any relevant operational settings (e.g., filter tape, inlet, flow rate, and reference MAC). Although each monitoring site was active for different periods, this study primarily focused on the period between 2017 and 2019 to evaluate the spatial variability of eBC mass concentration to 1) ensure that data was available from all sites and 2) to avoid the effects of the COVID-19 lockdowns. However, only sites that provided more than nine years of eBC observations and where at least 75% of the data was available were considered for trend analysis; as a result, the entire dataset can be used for subsequent epidemiological studies. It should be noted that missing data in the datasets were not gap-filled in further analyses. Various statistical measures were calculated for each site, including the minimum, maximum, 25th, 75th, and 99th percentiles, mean, median, and the number of data points per station. The overall dataset covers the period between 2006 and 2022, with single-site coverage ranging from a year to 14 years. Fig. S1 visualizes the distribution of eBC data available in the RI-URBANS dataset, including data coverage, data capture, and missing data from the various instruments. The blank area represents the missing data across the entire period. Aside from the low data coverage of some stations, the common period used in this study for the analysis and interpretation of the results (2017–2019), is fulfilled by majority of the sites.

The majority of the collected data were directly supplied by the data providers as hourly averages (Table S1). There are only two cases in which raw data with a native time resolution were provided; these data were averaged hourly for the purposes of this study. In some cases, EBAS Level 2 quality assured/quality checked (QA/QC) data were directly downloaded from the EBAS database (EBAS, https://ebas-data.nilu.no/). The data were processed following the ACTRIS recommendations for the reporting of eBC measurements (Müller and Fiebig, 2018a, 2018b), ensuring the comparability of eBC measurements across the sites by employing harmonized measurement protocols.

The procedure used to obtain particle light absorption coefficients—and consequently, eBC concentrations—from the available data is summarized in Fig. 2. The majority of the sites provided eBC concentrations that were used as is to analyze eBC variability. In cases where particle light absorption data were provided, the eBC concentrations were retrieved using default MAC values and the opportune harmonization factors H* as described in the following. Fig. 2 also presents the equations that were used to calculate the particle light absorption coefficients from the wavelength-dependent eBC concentrations provided by aethalometer instruments. These harmonized particle light absorption coefficients were then used in the aethalometer model for eBC source apportionment. As previously mentioned, AE33 instruments already correct online for factor loading, while data from older aethalometers (AE31 and AE22) were corrected offline by data providers. Specifically, the correction scheme proposed by Segura et al. (2016) was applied to the AE31 data from VLC_UB, while the scheme

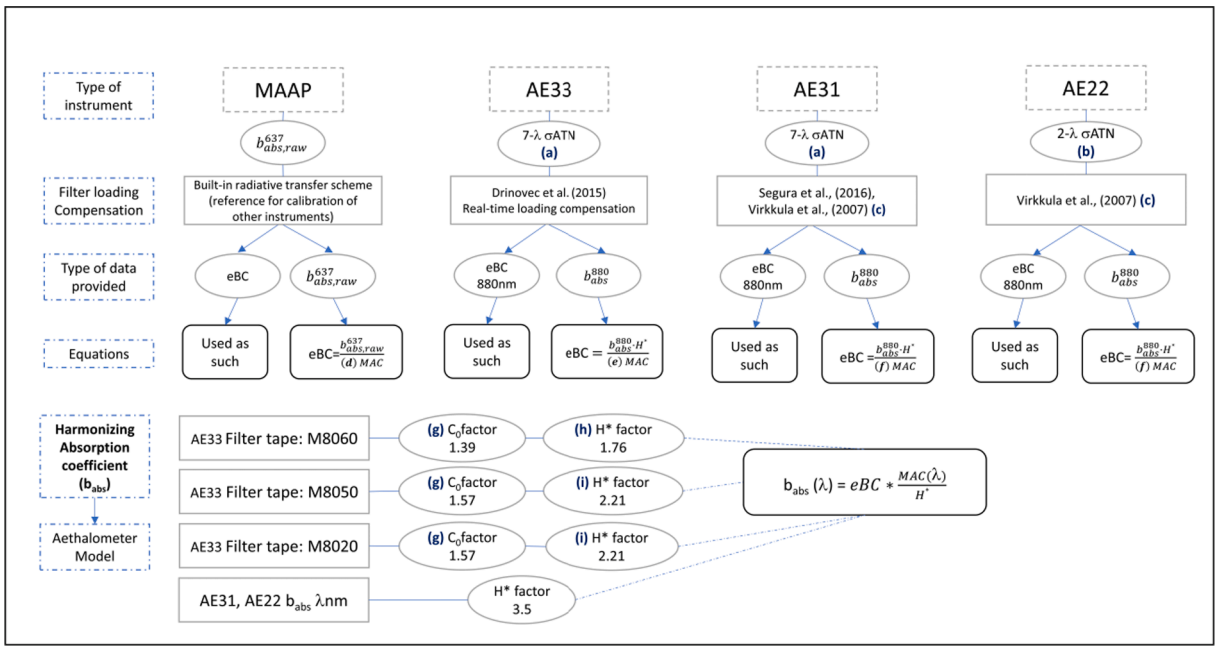

Fig. 2. The overall scheme by which to process corrected and harmonized eBC mass concentrations and absorption coefficients (b_{abs}) from the attenuation coefficient (σ_{ATN}). Data were supplied from different types of instruments and methods, which were then used in eBC source apportionment using the harmonized absorption coefficient (b_{abs}). More details are provided in section 2.3. (a) AE33 and AE31 wavelengths: 370, 470, 520, 590, 660, 880, and 950 nm; (b) AE22 wavelengths: 370 and 880 nm; (c) Offline filter loading correction algorithms: Segura et al. (2016) was used to correct the AE31 data from Valencia; Virkkula et al. (2007) was used to correct AE31 data from SMR_RB and correct AE22 data from LND_UB and LND_TR; (d) MAAP: MAC = 6.6 m^2/g at 670 nm; (e) AE33: MAC = 7.77 m^2/g at 880 nm; (f) AE31 and AE22: mass attenuation cross section = 16.62 m^2/g at 880 nm; (g) Default multiple-scattering enhancement correction factor used by the aethalometer software (1.39 or 1.57); (h) Harmonization factor (H*) for M8060 filter tape; (i) Harmonization factor (H*) for M8050 and M8020 filter tapes. M8050 was used for a short time and was not characterized; thus, processing was performed with the same harmonization factor as filter tape M8020.

proposed by Virkkula et al. (2007) was applied to the AE31 and AE22 data from SMR_RB and LND_UB/LND_TR, respectively (Fig. 2).

To calculate the particle absorption coefficients from aethalometer instruments, two parameters that depend on the type of aethalometer and filter tape used must be considered: the default multiple-scattering enhancement parameter (C_0) and the standardized harmonization factor (H*) provided by ACTRIS (Müller and Fiebig, 2018a). For AE33 instruments, the C_0 is manually set using the instrument software and should be changed depending on the filter tape used. Three different filter tapes were used across the monitoring sites: the M8020 (also known as TFE-coated fiberglass tape or T60A20), which was employed from approximately 2011 until February 2016; the M8050, which was used between February 2016 and October 2017; and the recently recommended M8060 filter tape, which has been in use since October 2017. The default C_0 values are 1.57 for both M8020 and M8050 and 1.39 for the new M8060 filter tape. However, recent studies have shown that these default C_0 values were not appropriate; thus, H* factors were introduced to standardize the calculation of the absorption coefficients. ACTRIS proposed an H* value of 1.76 for M8060 filter tape, while the proposed H* value for the AE33 M8020 and M8050 filter tapes was 2.21 (Müller and Fiebig, 2018a). Currently, guidelines from the Global Atmosphere Watch Programme suggest the use of H* = 3.5 for AE31 and AE22 (WMO/GAW, 2016). Thus, it is crucial to have the information about the filter tape used as well as the default C_0 to apply these corrections appropriately.

It should be considered that H* can vary depending on the physical properties of particles collected on the filter tape. For example, Yus-Díez et al. (2021) showed that the C_0, and consequently the H*, increases when the single scattering albedo (SSA) of collected particles is high (>0.95). Yus-Díez et al. (2021) observed this effect, known as cross-sensitivity to scattering, at two remote/regional background sites but did not observe it at the urban site, where the SSA was low. Thus, the assumption of a constant H* is reasonably correct at the urban/traffic sites included in this work.

As previously mentioned, we have presented the eBC concentrations as calculated according to the default MAC values provided by the manufacturers as this is the common practice in monitoring networks (cf. Fig. 2). However, it should be acknowledged that numerous studies have shown that the MAC can vary between different sites as well as over time depending on the physicochemical properties of the eBC particles (Cho et al., 2019; Ciupek et al., 2021; Grange et al., 2020; Knox et al., 2009; Kondo et al., 2009; Mbengue et al., 2021; Srivastava et al., 2022; Wu et al., 2021; Yuan et al., 2021; Zanatta et al., 2016; Zhao et al., 2021).

Thus, it should be noted that the comparability of eBC data reported in this study is partially affected by instrument-to-instrument variability. For example, Müller et al. (2011) reported a unit-to-unit variability of<5% for MAAP instruments while noting a variability of up to 30% for old aethalometer models, such as the AE31. This large variation was primarily associated with sample flow, spot size, and the inadequacy of current correction functions. As previously mentioned, AE31 data needs to be corrected off-line for factor loading effects, thus contributing to the higher noise inherent in AE31 data compared to MAAP data. For example, Asmi et al. (2021) reported a difference of about 7% between MAAP and AE31 data with a low correlation (R^2 = 0.65); in contrast, the correlation between MAAP and AE33 instruments was much higher (R^2 = 0.87). Additionally, Helin et al. (2018) reported a good correlation (R^2 > 0.90) between MAAP and AE33 data, with AE33 instruments reporting slightly higher concentrations. Recently, Cuesta-Mosquera et al. (2021) reported on the relatively small unit-to-unit variability of AE33-based eBC measurements, ranging between –16% and 8% with an average deviation of around –1% for soot. In most cases, the deviations could be explained by the type of filter material employed by the instruments, the total particle load on the filter, and the flow calibration. To reduce the instrument-to-instrument variability of AE33, Cuesta-Mosquera et al. (2021) recommended the use of the most

recent version of filter tape (M8060) while avoiding the use of older filter tapes. Furthermore, they highlighted the importance of reporting not only the filter tape used but also the corresponding multiple-scattering parameter C_0 set by the internal aethalometer settings. Due to its high accuracy and low uncertainty (12%; Petzold et al., 2005), the MAAP is considered to be the ideal reference instrument for the calculation of particle light absorption coefficients. Thus, we used eBC data from the MAAP instruments in stations where other filter absorption photometers were simultaneously deployed (IPR_RB, SMR_RB, BCN_UB, and GRA_UB).

Long-term trends were studied using three different approaches. The first approach involves the use of a Theil-Sen slope regression estimator: a robust, reliable, and non-parametric estimator provided in the Openair R package (Carslaw and Ropkins, 2012). This method assesses long-term trends by calculating monthly means as derived from hourly measurements. This approach not only enables the determination of statistical significance but also facilitates the estimation of slope values for the identified trends. As previously mentioned, only monitoring sites with a minimum of nine years of eBC mass concentration data with at least 75% valid measurements over that period were used in these analyses. It is important to note that some sites experienced changes in the measurement methodology over the nine-year period, most commonly due to changes in the filter-based instruments being deployed (e.g., shifting from MAAP to AE33 or from AE31 to AE33). Thus, the trends in absorption measurements can be influenced by the change in signals due to different instruments in 3 out of 13 sites (e.g., ZUR_UB, BER_UB, and SIR_SUB). Theil-Sen method was primarily used for inter-annual trend analysis. However, it does not take the shape of trends and possible breakpoints into account. Thus, the shape of trends and their seasonal variations were investigated through the more widely used decomposition method, a seasonal-trend decomposition time series procedure (STL) based on the 'Loess' estimator (Cleveland et al., 1990). The STL method is a powerful and versatile approach for analyzing time series data, allowing for the extraction of trends and seasonal components while accounting for various data characteristics and patterns. 95% confidence intervals calculated using bootstraps are also provided for the STL and Theil-Sen results. Another approach to investigate the presence of potential breakpoints that split the trends into segments with different slopes was piecewise regression using the "segmented" package (Muggeo, 2003, 2008). To estimate the slope and statistical significance of each segment between breakpoint positions, an interactive procedure that involves approximate starting values for the breakpoints and a bootstrap restarting methodology was implemented to enhance the robustness of the analysis and obtain standard errors (Wood, 2001). By using this procedure to fit a piecewise regression model, we were able to effectively characterize and interpret the distinct trends observed in the eBC data. This approach provided valuable insights into the changes and shifts in eBC mass concentration, allowing for a comprehensive analysis of the behavior of the data over different segments.

2.4. Aethalometer model and source apportionment

To evaluate the relative contributors of eBC_T and eBC_{RC} at the RI-URBANS sites, an aethalometer model was employed; this uses the multi-wavelength absorption data obtained from the AE33 following a procedure initially developed by Sandradewi et al. (2008a). Briefly, the model uses a bilinear method to estimate both eBC sub-fractions. This model has been widely applied and used by numerous investigators, discriminating between mostly traffic (notably including diesel, gasoline and natural gas combustion) and residential and commercial (biomass or coal combustion) eBC components (Becerril-Valle et al., 2017; Favez et al., 2010; Grange et al., 2020; Harrison et al., 2013; Helin et al., 2018; Tobler et al., 2021; Virkkula, 2021). The AE model was applied using 23 AE33 datasets taken from the RI-URBANS database. The source apportionment analysis used time series data between 2017 and 2019. The aethalometer model uses pre-defined source-specific absorption Ångström exponents (AAEs) as recommended by Sandradewi et al. (2008a) and Zotter et al. (2017).

The AAE is an optical parameter that describes the spectral dependence of light absorption by aerosols. It has been intensively employed for eBC source apportionment and aerosol characterization (e.g., BC, Brown Carbon "BrC", and dust) (Garg et al., 2016; Li et al., 2016; Liu et al., 2018; Wang et al., 2021; Zhang et al., 2019a; Zhang et al., 2019b). An AAE of around 1 indicates that the absorption is dominated by BC; a progressive increase in AAE is associated with an increasing contribution from non-BC absorbing components such as BrC or mineral dust (Zhang et al., 2020a, 2020b). The application of the aethalometer model requires a priori knowledge of the AAE of the main sources of BC. Values of around 1 and 2 for the two wavelengths of 470 and 950 nm are commonly used for traffic and residential, commercial sources (e.g., biomass burning and coal combustion), respectively (Sandradewi et al., 2008a). More recent estimates based on ^{14}C analysis have suggested values of 0.90 and 1.68 (Zotter et al., 2017). However, both AAE values may vary significantly depending on the type of fuels being burnt, burning conditions, and the microphysical properties of the BC particles (the size of the BC particle and internal mixing with non-absorbing or less absorbing material): a single value cannot be representative of the whole measurement period considered (Helin et al., 2021; Li et al., 2016; Liu et al., 2018). For this reason, the aethalometer source apportionment model is associated with uncertainties related to fixed specific AAEs of traffic-related and residential and commercial emission sources [AAE_T and AAE_{RC}] (Harrison et al., 2013; Helin et al., 2021; Zotter et al., 2017).

Thus, the selection of robust AAE values is a critical component of the aethalometer model and has been validated in previous studies using ^{14}C observations as well as other auxiliary measurements such as Elemental Carbon, Organic Carbon (EC/OC) (Sandradewi et al., 2008a; Sandradewi et al., 2008b; Zotter et al., 2017). This study follows the conventional approach of using fixed AAE values for the source apportionment of AE33 observations due to the lack of ancillary measurements (such as ^{14}C measurement data) that could be used to determine site-dependent AAEs. Thus, AAE values of 1 and 0.90 were used for eBC_T, while AAE values of 2 and 1.68 were used for eBC_{RC} for the wavelengths of 470 nm and 950 nm, respectively. The results obtained were compared to evaluate the variations across different regions due to the limitation of constant AAE values.

3. Results and discussion

3.1. Overview of eBC observations and average eBC mass concentrations

This section reports the measurement data collected using different filter-based techniques at 50 European sites. Table S2 presents the statistical analysis of the eBC mass concentration at each site using hourly averaged data recorded between 2017 and 2019. Specifically, the mean, maximum, minimum, and standard deviation were calculated for each site. Data coverage information and mean concentration values for spring (MAM), summer (JJA), autumn (SON), and winter (DJF) are also presented in Table S2.

The box-and-whisker plots in Fig. 3 describe the variability of eBC mass concentrations in different regional sectors based on hourly averaged data from the relevant stations during the study period (2017–2019). Overall, the changes in concentrations reflect an increasing trend from north to south, with values ranging from 0.71 μg m^{-3} (North) to 1.70 μg m^{-3} (South). The relative contribution of different sources to these concentrations is discussed in Section 3.2. The results revealed that eBC mass concentrations decreased in different sampling locations as follows: TR > UB > SUB > RB. Notably, IPR_RB deviated from the observed trend, exhibiting high eBC concentrations (1.4 ± 1.5 μ gm^{-3}), due to its location within the Po Valley PM hotspot (Gilardoni et al., 2020; Masiol et al., 2020; Mousavi et al., 2019; Sandrini et al., 2014). The high concentrations at IPR_RB emphasize the

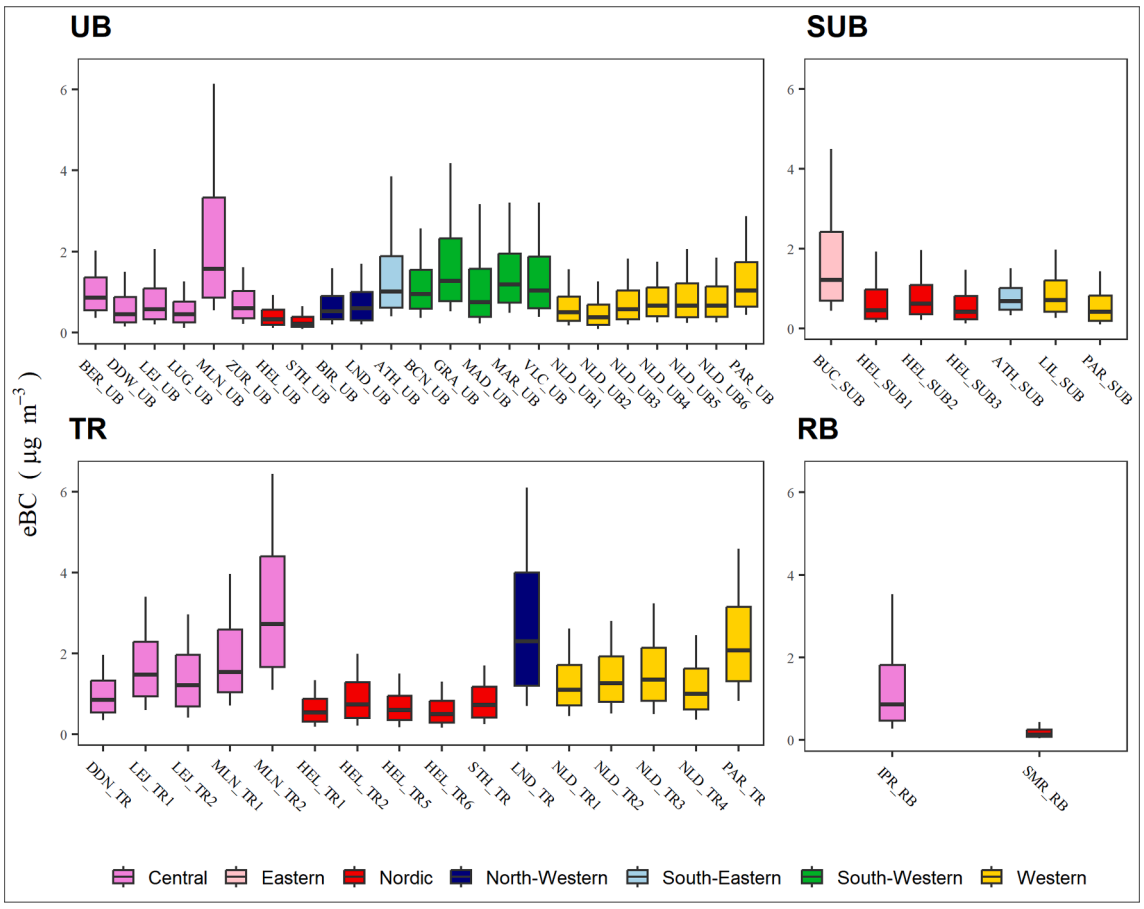

Fig. 3. The variability of hourly averaged eBC mass concentrations at 50 sites between 2017 and 2019 categorized by the type of site and region. In the box and whisker plots, each box represents the range between the first and third quartile with the median value for each season represented by the inner line. The whiskers extend to the minimum and maximum values as determined by the 10th and 90th percentiles.

significant influence of meteorological conditions on eBC mass concentrations, as these readings are considerably higher than those at other UB or TR sites in Central Europe.

Furthermore, a decreasing trend in mass concentrations in the UB sites was observed moving from the Western and South-Western regions to Central and Northern Europe with the highest eBC mass concentrations reported for MLN_UB (2.5 ± 2.5 μg m^{-3}) and GRA_UB (1.9 ± 2.0 μg m^{-3}). At TR sites, lower concentrations are observed in the Northern regions compared to Central Europe. The results showed that there were significant disparities in eBC concentrations between the sites, with the highest eBC mass concentrations reported for MLN_TR2 (3.4 ± 2.3 μg m^{-3}) and LND_TR (2.9 ± 2.2 μg m^{-3}).

The absence of eBC measurements from Eastern Europe and the lack of measurements from TR sites in Southern Europe are clearly shown in Fig. 3. These limitations may affect the comprehensive assessment of spatiotemporal variability of eBC mass concentrations across Europe. Our primary focus in this study is to identify similarities and differences between the different European sites, rather than one-site peculiarities, which will be examined and discussed in detail in this section. As documented in prior studies on European aerosol phenomenology, meteorology, and regional geography can lead to significant differences in concentrations of pollutants such as eBC (Cavalli et al., 2016; Putaud et al., 2004; Van Dingenen et al., 2004). The greatest site-by-site variability in eBC mass concentrations for both the UB and TR sites was observed in Central Europe. The mean eBC concentrations at the TR sites (1.6 ± 1.2 μg m^{-3}) between 2017 and 2019 were higher than those measured at UB sites (1.3 ± 1.4 μg m^{-3}). The lowest mean concentration observed among the TR sites was 0.67 ± 0.68 μg m^{-3} in HEL_TR6, while the highest was 3.4 ± 2.3 μg m^{-3} in MLN_TR2. The eBC mass concentration in MLN_TR2 and LND_TR were relatively similar, while MLN_UB exhibited elevated eBC levels. In contrast, the eBC mass concentration at LND_UB was significantly lower. The LND_TR monitoring station is located on the kerbside of a street canyon (Marylebone Road), which is an area of the city that experiences heavy traffic (Rivas et al., 2020). Thus, local traffic was the main source of air pollution on this site (Ciupek et al., 2021). Similarly, because of its specific geographic location within the Po Valley (with extremely low winds and frequent atmospheric stagnation episodes), Milan is recognized as a regional pollution hotspot in Europe (Mousavi et al., 2019; Sandrini et al., 2014). Consequently, it has been characterized as a high-density polluted urban area dominated by traffic and biomass-burning sources that have been previously associated with elevated eBC mass concentrations (Invernizzi et al., 2011; Mousavi et al., 2019). In PAR_TR (located in Paris, the second largest city in Europe), the mass concentration of eBC (2.5 ± 1.7 μg m^{-3}) is significantly impacted by primary emission sources, particularly traffic (Crippa et al., 2013; Favez et al., 2009). Conversely, the contribution of biomass-burning to eBC is relatively low at this station (Laborde et al., 2013).

In general, the recorded variations at UB sites ranged from a low of 0.3 ± 2.9 μg m^{-3} at STH_UB to a high of 2.5 ± 2.5 μg m^{-3} at MLN_UB. GRA_UB also exhibited high eBC mass concentrations (1.9 ± 2.0 μg m^{-3}), likely due to its location in a narrow valley, as well as the open burning of wood and strong and frequent thermal inversion during the cold months (Titos et al., 2017). Among the SUB sites, the highest eBC mass concentrations were observed at BUC_SUB (2.1 ± 3.0 μg m^{-3}), primarily due to the influence of noticeable biomass-burning during summer (Chen et al., 2022). The lowest eBC mass concentration among all sites was reported at SMR_RB (0.2 ± 0.20 μg m^{-3}) and STH_UB (0.3

± 0.3 μg m^{-3}). STH_UB is affected by wood smoke emissions during wintertime (Krecl et al., 2011), while SMR_RB—a rural station—typically experiences one of the lowest eBC loads in Europe (Hyvärinen et al., 2011; Yttri et al., 2011). The ranges of eBC mass concentrations described above also reflect the diverse environmental conditions across Europe, including variations in meteorology and urban and regional emissions patterns (Bressi et al., 2021).

In the context of eBC mass concentrations within specific regions, a relatively low degree of site-by-site variability was observed at TR sites in the Northern countries. Comparatively, the regions of Western (Netherlands) and Northern (Finland) Europe exhibited noticeably lower eBC mass concentrations compared to other urban areas across Europe. Finland's geographical isolation from the more densely populated regions of Europe due to their separation by the Baltic Sea results in the reduced influence of long-range pollution originating from the more polluted areas (Luoma et al., 2021). In Northern Europe, biomass-burning emissions have been identified as a significant source of air pollutants (Helin et al., 2018; Hienola et al., 2013; Hyvärinen et al., 2011; Luoma et al., 2021). Our results showed that the higher eBC concentrations observed at the Northern SUB sites are consistent with previous studies that have highlighted increased eBC contributions from residential wood and other biomass combustion during the cold seasons in the SUB area (Helin et al., 2018; Luoma et al., 2021). In general, low site-by-site variability was observed in both SUB and RB sites in Northern countries. Northern countries can thus be characterized by their low eBC concentrations and site-by-site variability.

The variability of eBC concentrations at Western European TR sites was found to be higher than at UB sites. Schaap and Denier van der Gon (2007) previously demonstrated that TR stations in the Netherlands exhibited greater variability in eBC concentrations compared to UB and RB sites. For instance, the relatively high eBC mass concentrations in Rotterdam (NLD_TR3; 1.7 ± 1.2 μg m^{-3}) were mainly attributed to high road traffic emissions (Keuken et al., 2009).

Data was only available at three stations in South-Eastern and Eastern European countries, limiting the efficacy of site-by-site variability analyses in these particular regions. However, these stations can still be compared to other EU regions. Notably, BUC_SUB (2.1 ± 3.0 μg m^{-3}) reported significantly higher eBC mass concentrations compared to similar sites in other regions. ATH_SUB is affected by both traffic and residential and commercial combustion sources (Diapouli et al., 2017). However, the eBC concentrations at ATH_UB (1.7 ± 2.2 μg m^{-3}) were comparable to other UB sites in Southern Europe and exhibit values that are nearly double than those observed at ATH_SUB (0.80 ± 0.5 μg m^{-3}), suggesting that there is significant spatial variability in ambient eBC and its emission sources in Athens (Grivas et al., 2019; Kaskaoutis et al., 2021).

In South-Western Europe, GRA_UB exhibited higher eBC mass concentrations compared to other sites, potentially influenced by meteorological patterns, orographic factors, and high biomass-burning emissions (Titos et al., 2017; Van Drooge et al., 2022). The eBC mass concentrations at VLC_UB, BCN_UB, and MAR_UB were similar, while the lowest eBC mass concentration was recorded at MAD_UB due to the least influence from traffic in this site. However, studying the variability of long-term measurements of eBC mass concentrations at the European scale is challenging since the characterization of eBC mass concentration by station is restricted due to significant regional variability.

It should be noted that intense desert dust episodes (DDE) can also contribute to the measured absorption and can thus affect the calculated eBC concentrations. The contribution of this dust to absorption measurements has been most commonly observed at remote sites where eBC concentrations are usually low (e.g., Ripoll et al., 2015). However, at urban sites where eBC is expected to dominate absorption, the impact of DDE on eBC concentrations is relatively insignificant, as can be seen by the relationship between eBC and NO_2 concentrations at BCN_UB over three years of data (see Fig. S2). It should also be noted that DDE events are sporadic, thus further reducing the influence of DDE on urban sites over long timescales such as those used in this study.

3.2. Source apportionment analysis of eBC

The aethalometer model was applied to 23 AE33 datasets at seven wavelengths; the results of this analysis are presented here. This model was used to determine the relative contribution of eBC_{RC} and eBC_T to bulk eBC based on the particle light absorption coefficients calculated over the entire study period (2017–2019). The mean concentrations of eBC_T and eBC_{RC}, as well as their corresponding standard deviations, were determined using hourly averaged data at different sites during the study period and are reported in Table S3 (using $AAE_T = 1$ and $AAE_{RC} = 2$) and Table S4 (using $AAE_T = 0.90$ and $AAE_{RC} = 1.68$). Fig. 4 shows the results of the aethalometer source apportionment model in Europe for $AAE_T = 1$ and $AAE_{RC} = 2$ (Sandradewi et al., 2008a). It shows the regional variations in the relative contributions of eBC_T and eBC_{RC} with an increasing trend in the relative contribution of eBC_T from Northern to Central, Western, and South-Western Europe. The outcomes of the source apportionment analysis are summarized in Fig. 5, which provides a comparison of the relative contributions of eBC_T and eBC_{RC} between the TR and the UB/SUB sites using stacked histograms; the error bars indicate the respective variances of the two sources. These comparisons are presented using pie charts in Fig. 4. It shows that eBC_T had consistently higher relative contributions compared to eBC_{RC}. The highest relative contribution of eBC_T was obtained in PAR_TR (88%), STH-TR (87%), and MLN_TR (82%) sites. However, there were some regions and sites at which eBC_{RC} contributions were also relatively high.

Previous research has shown that eBC mass concentrations are predominantly influenced by residential and commercial combustion sources—particularly wood burning—during heating seasons (Crilley et al., 2015; Herich et al., 2011; Zhang et al., 2020a, 2020b, 2020c). The greatest relative eBC_{RC} contribution was observed at BUC_SUB (39%), the HEL_SUB sites (30–34%), GRA_UB (30%), BER_UB (27%), and MLN_UB (26%). The lowest eBC_T contributions were observed in Eastern Europe, while the highest contributions were recorded in Central and Western Europe (88%, 82%, and 74% at PAR_TR, MLN_TR2, and MLN_UB, respectively). It is worth noting that the relative contribution of eBC_T in the Northern TR sites was much lower compared to TR sites in Western Europe, such as PAR_TR, with the exception of the UB and TR sites of MLN in Central Europe. In contrast, in South-Eastern Europe, both ATH_UB and ATH_SUB exhibited higher relative contributions of eBC_T despite being recognized as hot spots for residential wood burning, especially during winter (Kaskaoutis et al., 2021; Liakakou et al., 2020). There was a clear decreasing trend in eBC_{RC} contributions from Northern to Central and Southern Europe. In Central, Eastern, and Northern Europe, the relative contribution of eBC_{RC} to eBC was found to be higher compared to other regions (39% in BUC_SUB, 30–34% in HEL_SUB sites, and 26% in MLN_UB). This pattern may be due to the increased emissions of solid fuel from residential areas during the cold season in these particular regions.

The higher relative eBC_{RC} contributions in South-Eastern Europe (ATH sites) during winter are likely attributed to the burning of wood for heating purposes (ATH_UB 31%, ATH_SUB 24%). Consequently, the ratio of biomass to fossil-fuel combustion emissions in this region was higher in winter, particularly on weekends (Kaskaoutis et al., 2021; Merabet et al., 2019). The SMR_RB station is mainly affected by regionally sourced and long-range transported pollutants in Northern Europe (Hyvärinen et al., 2011). In addition, the SMR_RB station may be affected by the surrounding station buildings as well as the city of Tampere itself (Yttri et al., 2011). In the Helsinki region, stations HEL_SUB1 to HEL_SUB3 are located in detached housing areas that are affected by the utilization of fireplaces for wood burning in winter (32% relative contribution to eBC_{RC}) in addition to road traffic emissions (Helin et al., 2018; Fung et al., 2022). STH_TR, located in the city center, is heavily influenced by traffic emissions (75% eBC_T) (Krecl et al., 2011;

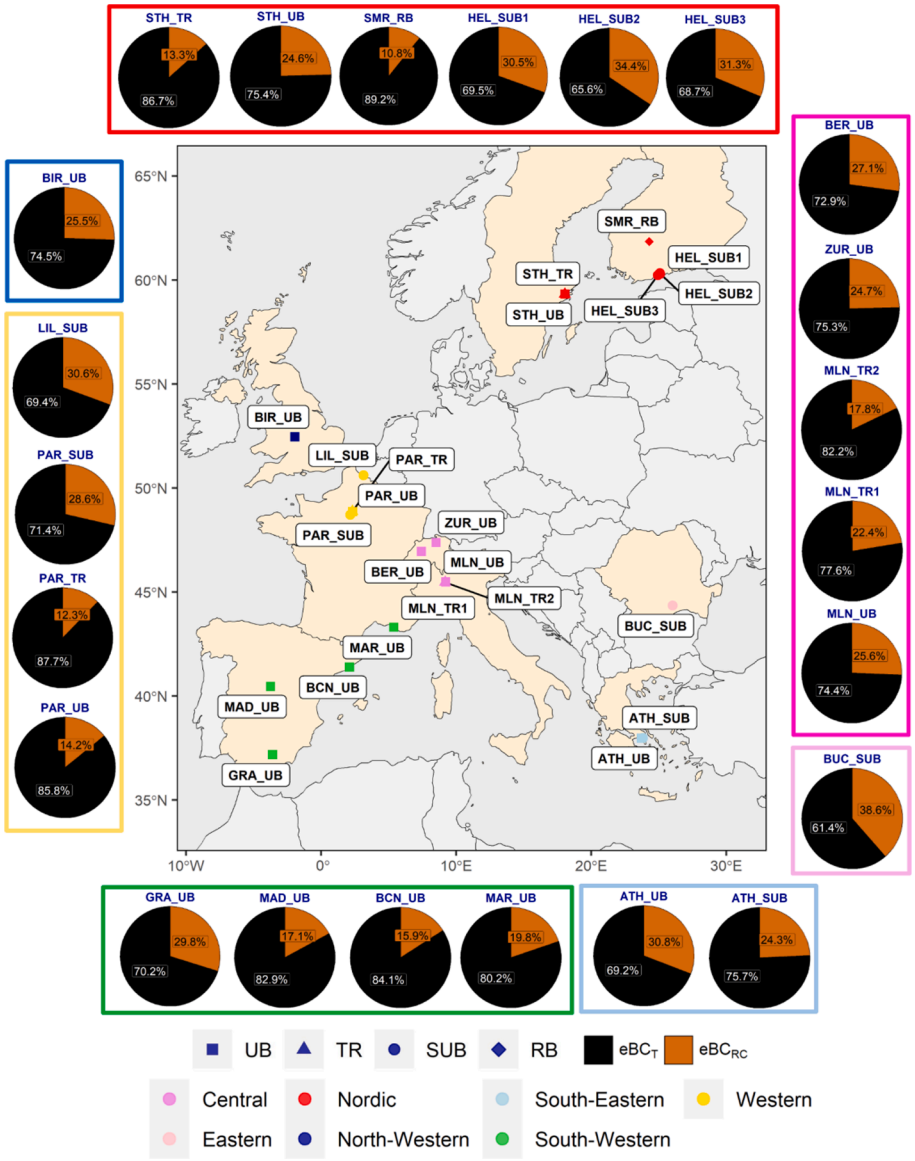

Fig. 4. The results of the source apportionment analysis of eBC mass concentrations for 23 European sites used over the study period (2017–2019). The aethalometer model was applied using (AAE_T = 1) for traffic emission sources and (AAE_{RC} = 2) for residential and commercial emission sources. The colors highlight the geographic locations of the sites that supplied AE33 eBC data.

2017).

Of the South-Western UB sites, high contributions of eBC_T and eBC_{RC} were observed in BCN_UB (84%) and GRA_UB (30%), respectively. Similarly, MAD_UB (83%) and MAR_UB (80%) also exhibited high relative contributions of eBC_T, consistent with findings reported by Baldasano (2020). MAR_UB is located in the most important Mediterranean seaport and is consequently influenced by a substantial amount of industrial urban emissions (Chazeau et al., 2022; El Haddad et al., 2013; Salameh et al., 2018). In Western sites, high eBC_T and eBC_{RC} contributions were observed in sites that are influenced by heavy traffic and biomass burning, such as PAR_TR (88%) and LIL_SUB (31%), respectively. In particular, LIL_SUB is highly influenced by biomass-burning emissions during spring, autumn, and winter as previously reported by Cordell et al. (2016). A recent study conducted at the LIL_SUB site revealed that, during the winter season, a significant portion of the organic aerosols consisted of less oxidized fractions (LO-OOA), and has been identified as originating from aged biomass burning. The study suggests that approximately half of the organic aerosols generated during winter can be attributed to wood combustion (Chebaicheb et al., 2023). In North-Western Europe, BIR_UB exhibited a dominant contribution of eBC_T (74%) due to its higher traffic emissions compared to domestic heating; this was consistent with a previous study on the variations and level of the eBC_T contribution at BIR_UB by Singh et al. (2018). In general, the relative contribution of eBC_T and eBC_{RC} is influenced by the geographical location and the prevailing type of combustion source at each station.

Moreover, we performed a comparison of the relative contributions of eBC_{RC} and eBC_T using two sets of AAE values: 1 and 2, and the AAE values proposed by Zotter et al. (2017), as shown in Table S4. In general, the relative contribution of residential and commercial sources to eBC increased by 25–45% when using the Zotter values (see Fig. S3). It should be noted that the AAE values proposed by Zotter et al. (2017), were determined at Swiss sites that were strongly influenced by biomass-burning emissions. However, based on the available data, we cannot definitively conclude which AAE pair (1, 2 vs. 0.90, 1.68) was more appropriate for the sites considered in our study. It is reasonable to apply the Zotter AAE values at sites with similar characteristics to those used in Zotter et al. (2017). However, there are some concerns regarding the

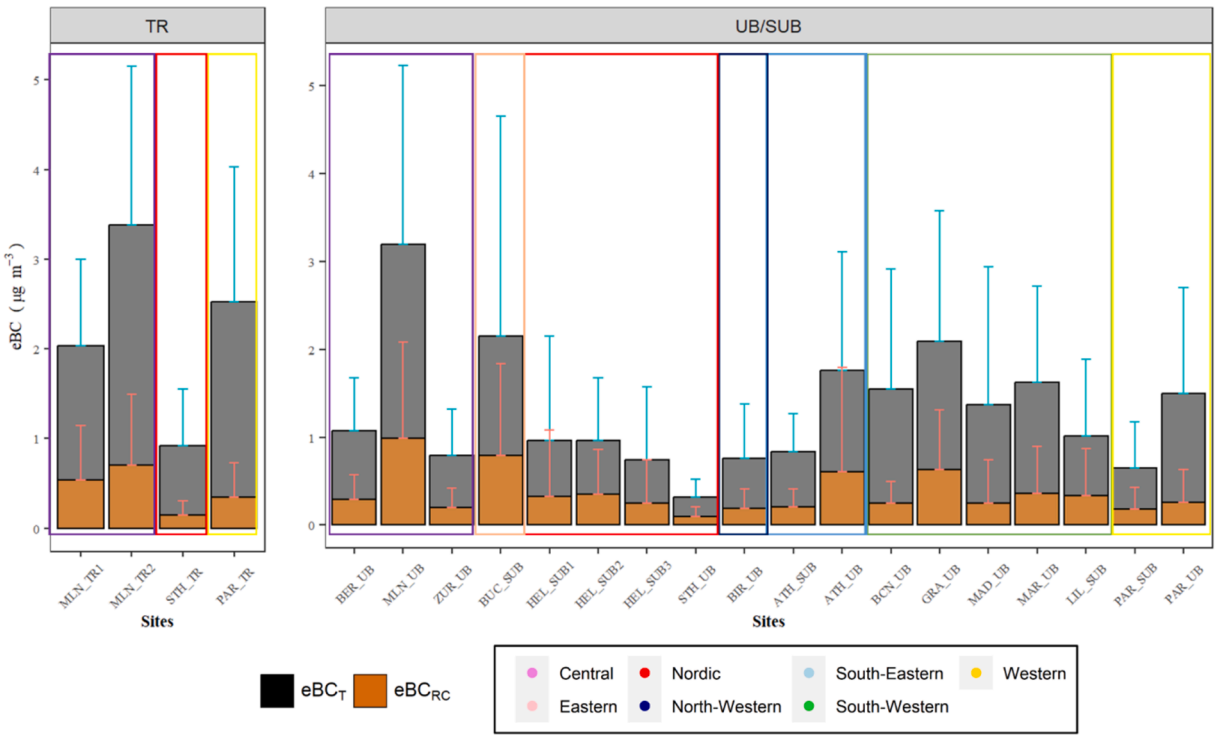

Fig. 5. The source apportionment analysis results of TR (traffic) vs UB/SUB (urban/suburban) sites. Stacked histograms with error bars were used to present the variance associated with the two sources based on geographic regions.

extensive use of Zotter values. For instance, in Barcelona, the Zotter values result in an excessively high contribution of eBC_{RC} to eBC (41% in winter), which contradicts recent studies demonstrating the very low contribution of biomass-burning to OA in this city (4–6% in winter; Via et al. 2021).

It thus cannot be assumed that the AAE values remain constant across all sites. To minimize these uncertainties, the use of site-specific AAE values is recommended; alternatively, a range of robust and consistent AAE values that accounts for the variability observed in the specific study area should be used. There are studies that have recommended the use of AAE frequency distributions as an alternative method to estimate site-specific AAE values (Tobler et al., 2021). Alternatively, the incorporation of time-dependent AAEs into the aethalometer model can be proposed, with the aim of evaluating its performance. In the next section, trends in eBC_T and eBC_{RC} will be analyzed to determine if there are stable patterns for eBC_{RC} and eBC_T in the data by considering monthly-deseasonalized average values for larger data series.

3.3. Seasonal variability

3.3.1. eBC seasonal pattern

Fig. 6 shows the average monthly variation in the total eBC mass concentrations across all sites between 2017 and 2019. In cases where monitoring sites provided eBC observations from multiple instruments, such as MAAP, AE31, and AE33, the analysis in this section primarily considers the seasonal variability observed from MAAP data. The priority in the use of specific instrument data was as follows: MAAP > AE33 > AE31 > AE22. The eBC mass concentrations were noticeably higher during winter (DJF) at a majority of sites, which may be attributed to the seasonal variability of eBC emission sources and meteorological conditions. In general, winter periods are characterized by lower mixing layer heights, lower wind speeds, and enhanced atmospheric stability, which contribute to the greater accumulation of pollutants, even in the presence of frequent precipitation (Cassee et al., 2019). In addition, higher winter domestic heating emissions contribute to increased eBC (Minderytė et al., 2022). The trend of higher eBC concentrations during winter has been already described in numerous studies (Becerril-Valle et al., 2017; Herich et al., 2011; Jing et al., 2019; Lyamani et al., 2011; Merabet et al., 2019; Pandolfi et al., 2014; Titos et al., 2017). The observed high winter eBC patterns are consistent with similar patterns of high winter NO_X and CO reported in many European and US studies, as both of these tracers are also emitted in large quantities by road traffic (Grange et al., 2021; Helin et al., 2018; Karagulian et al., 2015; Mousavi et al., 2018).

There are some cities where this seasonal cycle is not as pronounced or even non-existent. For instance, at BCN_UB, the effect of atmospheric inversion is relatively weak and biomass-burning in winter only has a minor contribution to ambient PM levels (Amato et al., 2016). PM speciation studies conducted at BCN_UB revealed that levels of biomass-burning organic aerosol in winter were lower there than in other European sites (Via et al., 2021).

Seasonal variations in eBC mass concentration were relatively stable in several Northern European sites, particularly at HEL_TR1, HEL_TR2, and STH_TR. These sites all are located in Nordic street canyons, where local traffic is the dominant source of eBC throughout the year, and there is no significant contribution from local wood combustion at these sites (Krecl et al., 2011; Helin et al., 2018). In addition, the low mean height of the boundary layer and low wind speeds during the early summer morning rush hours leads to elevated eBC mass concentrations in Helsinki during summer (Barreira et al., 2021). Seasonal variations at the STH_TR site can also be affected by the abatement of traffic since traffic exhaust has been found the most important source in city of Stockholm (Segersson et al., 2017).

The UB and TR sites in Europe, predominantly concentrated in the Western and Northern regions, exhibit a less pronounced seasonal variability, particularly in the Northern countries. In contrast, both UB and TR sites exhibited pronounced high winter patterns in Central Europe. The spatial variability observed at the SUB and RB sites was further influenced by their geographic locations and their local climate/meteorology.

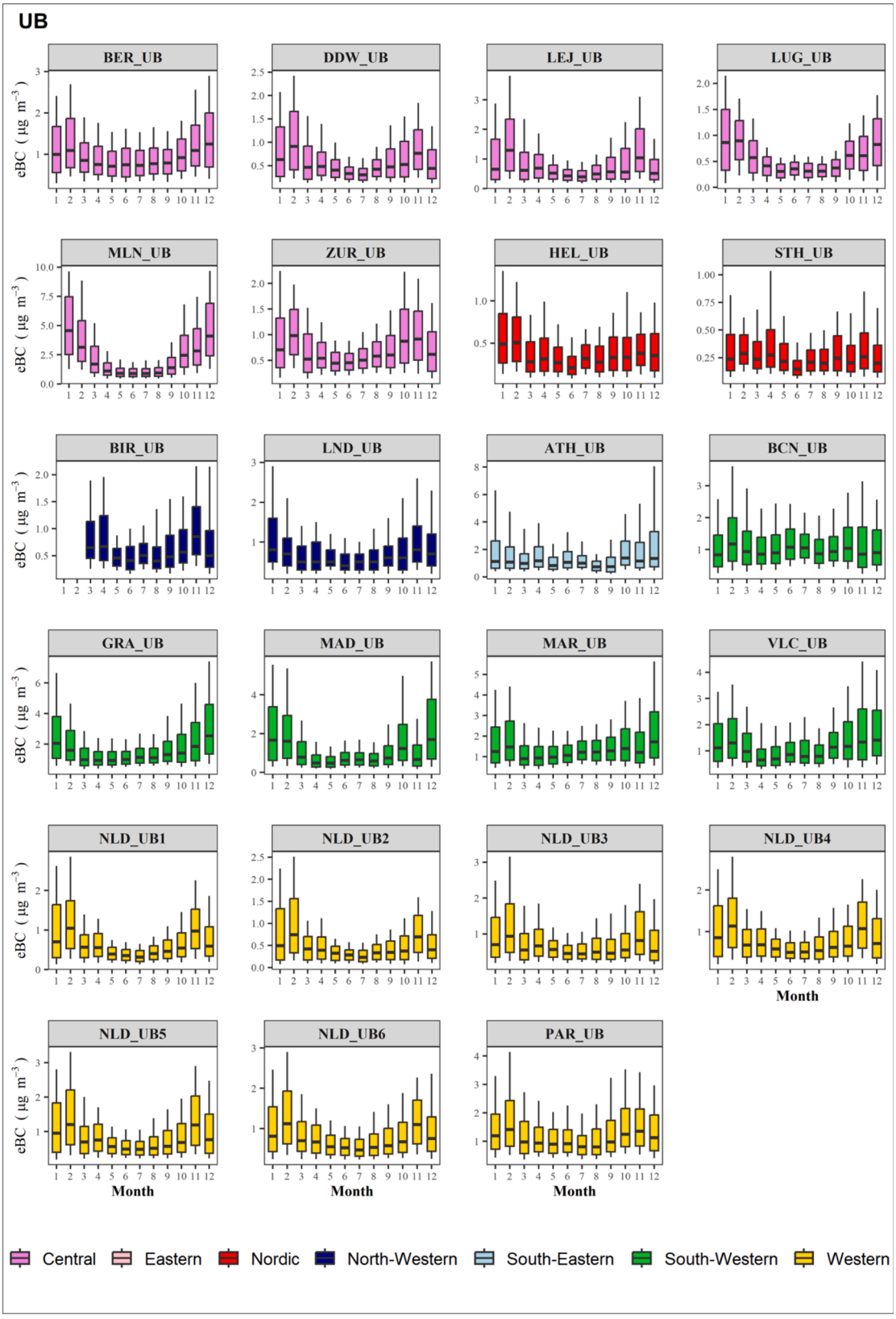

Fig. 6. The averaged monthly variability of eBC mass concentrations based on the type of site and region between 2017 and 2019. In box plots, the range of the box depicts the bounds of the 25th and 75th percentile of the data. The whiskers extend to the minimum and maximum values, determined by the 10th and 90th percentiles. The bold horizontal inner line shows the median for each month. The shaded background colors in box plots represent geographic locations.

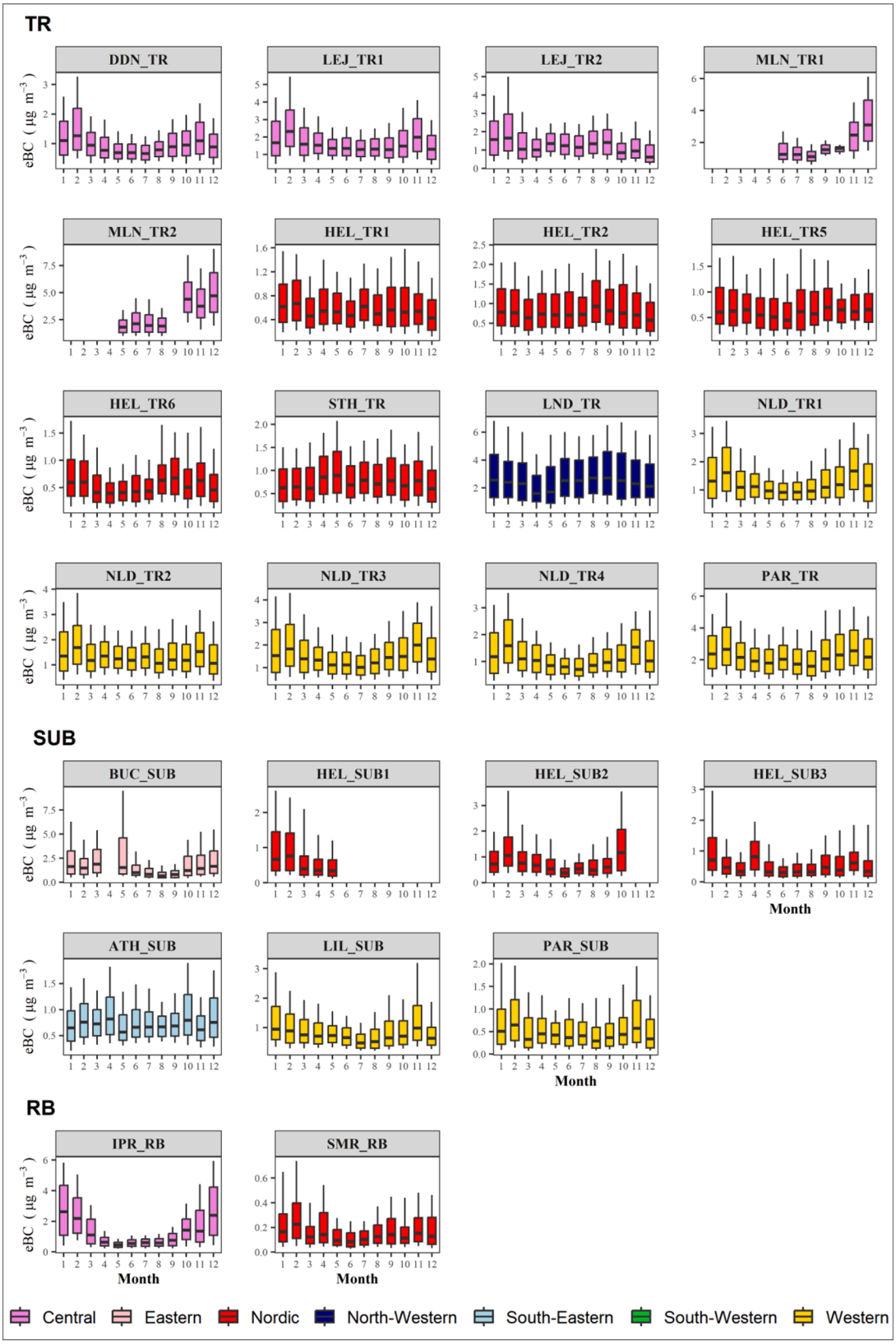

Fig. 6. (*continued*).

3.3.2. *Seasonal trends in eBC_T and eBC_{RC}*

The monthly variations of eBC_T and eBC_{RC} are presented in Fig. 7. In general, the results revealed that eBC source contributions exhibited pronounced seasonality and a significant inter-annual fluctuation during the study period (2017–2019). This is supported by Fig. 7, which illustrates the high variability of eBC_{RC}/eBC_T ratios for all studied sites, which vary from 23 to 87% across Europe. These fluctuations may be a function of the distance of the site to its traffic, residential, and

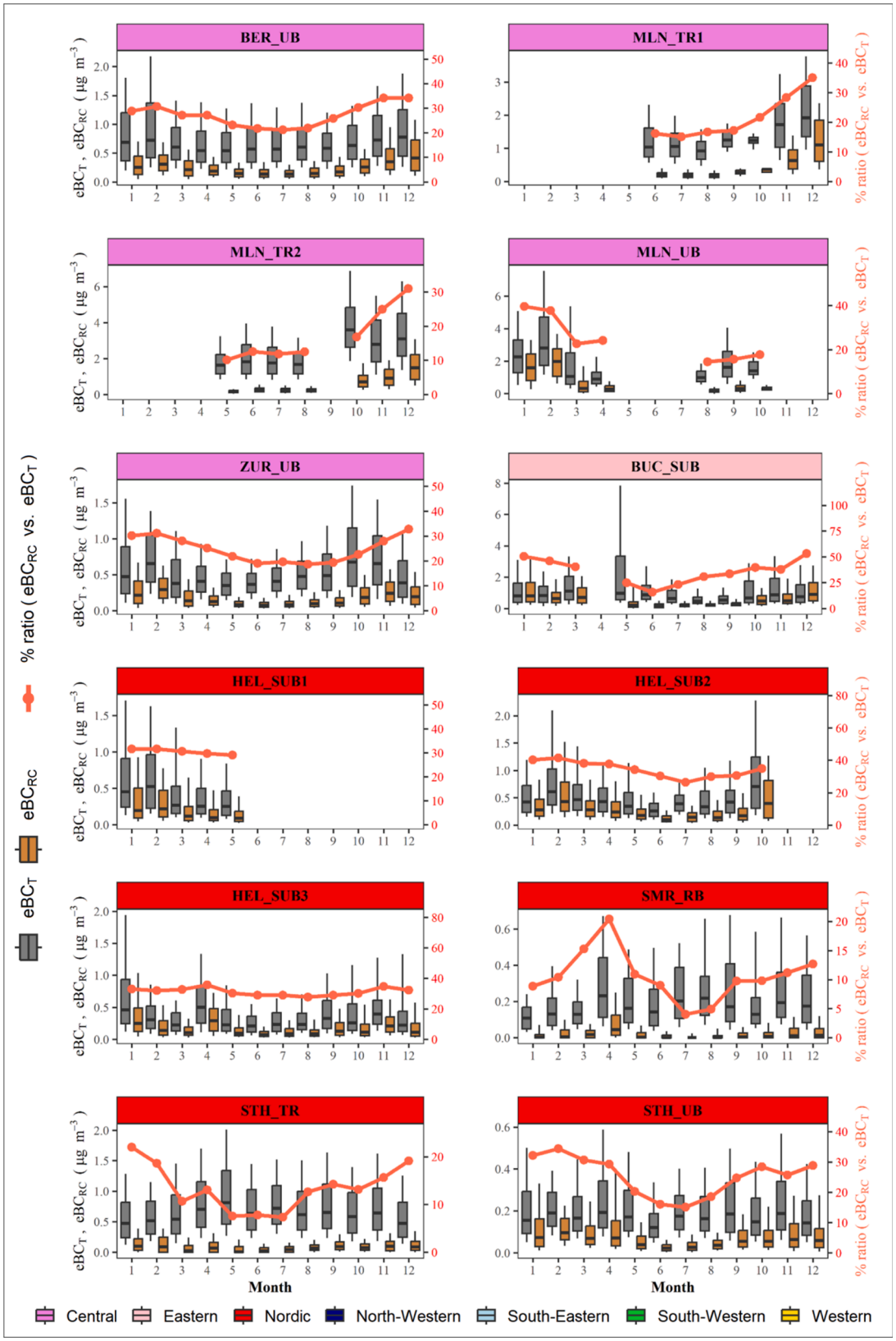

Fig. 7. The averaged monthly variability of eBC_T and eBC_{RC} concentrations based on the type of sites and region between 2017 and 2019. In boxplots, each box represents the range between the first and third quartile with the median value for each season distribution represented by the inner line. The whiskers extend to the minimum and maximum values, determined by the 10th and 90th percentiles.

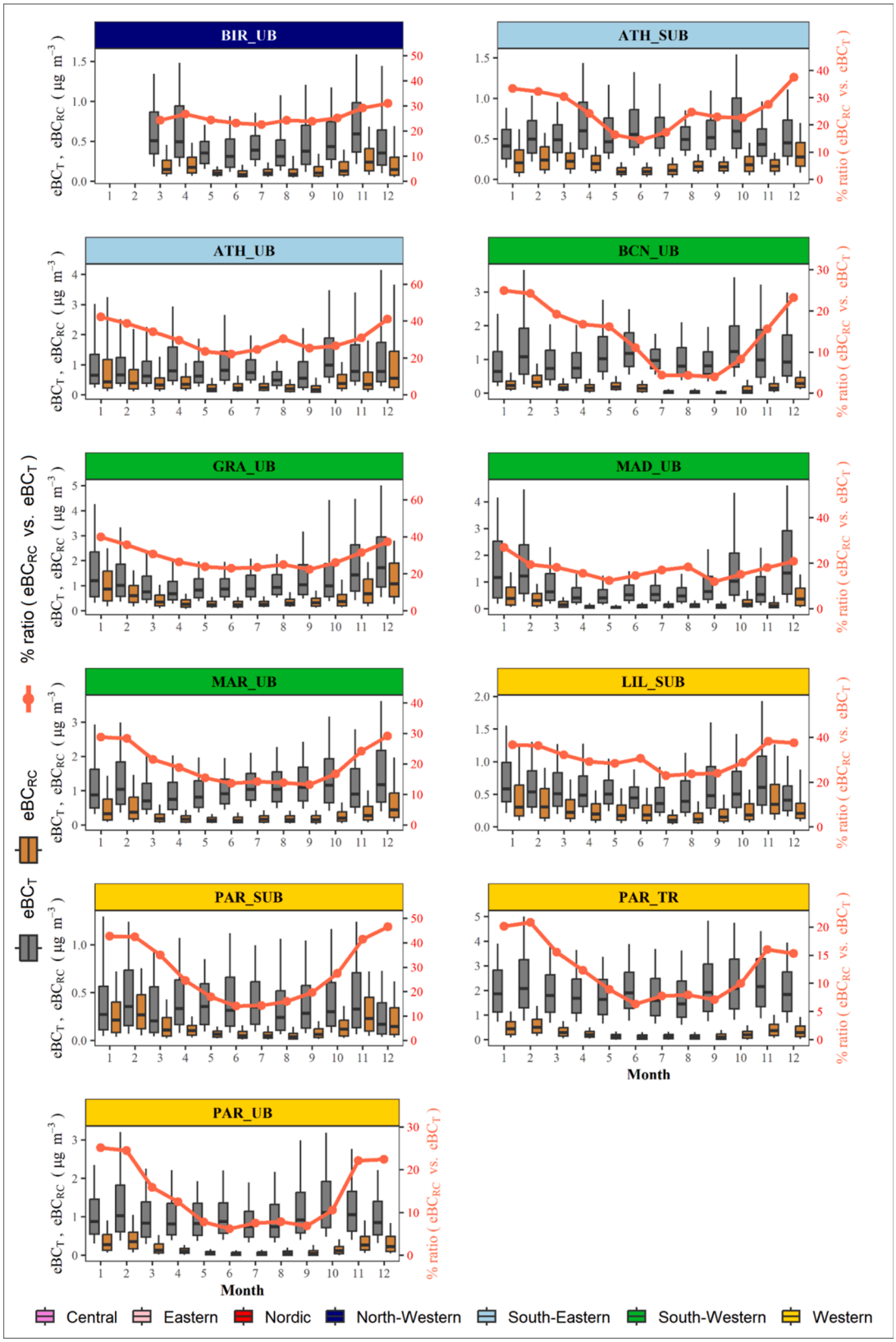

Fig. 7. (*continued*).

commercial source emissions, the relative influence of other emission sources, intra-annual variations in emissions from different combustion sources, and changes in meteorological conditions (Becerril-Valle et al., 2017; Bond et al., 2013; Helin et al., 2018; Kaskaoutis et al., 2021; Luoma et al., 2021; Zioła et al., 2021).

These observations are consistent with the decrease in the ratio of eBC_T/eBC_{RC} emissions during winter and their corresponding increase during summer (Hopke et al., 2022; Rigler et al., 2020; Rivas et al.,

2021), a trend that was also observed in this study for most UB/TR sites. Conversely, the eBC_{RC}/eBC_T emission ratio was expected to exhibit the opposite pattern, decreasing during summer and increasing during winter (Fig. 7). The monthly variation and the relative contribution of eBC_T and eBC_{RC} sources across the different sites are also presented as a 100% stacked histogram (see Fig. S4), offering insights into the spatial distribution and dominance of specific source types. The values used for these histograms were determined through the application of the aethalometer source apportionment model at 23 different sites using $AAE_T = 1$ and $AAE_{RC} = 2$. The y-axis of the histograms refers to the relative contribution of each source category (as a percentage), while the x-axis indicates their monthly variation. The stacked bars refer to the relative contributions of eBC_T and eBC_{RC} sources for each site.

The relative eBC_T contributions increased during winter as a result of more stagnant atmospheric conditions and increased traffic emissions during this season. At the same time, there was an increase in eBC_{RC} contributions due to the emissions from domestic sources (e.g., heating). The seasonal variations in eBC_T were observed to be lower compared to eBC_{RC}; this discrepancy is related to the lesser degree of seasonal dependence exhibited by urban traffic flow compared to the seasonality of solid fuel combustions, such as biomass- and coal-burning, which are prevalent at most sites (Harrison et al., 2013; Martinsson et al., 2017). Furthermore, it is worth noting that residential heating activities can also contribute to local NO_X and eBC, such as at the detached housing areas around the HEL sites (Helin et al., 2018). In the context of seasonal variations, the contribution of eBC_T was at a maximum during winter (3.5 μg m^{-3}) at MLN_TR2, with notably elevated values also observed during the summer (2.0 μg m^{-3}) at the same site. In contrast, the lowest values of eBC_T (0.22 μg m^{-3}) were measured in both summer and winter at STH_UB. The seasonal patterns of eBC_{RC} were similar, with the maximum concentrations observed at MLN_UB (1.90 μg m^{-3}) and MLN_TR2 (1.65 μg m^{-3}) during the winter and the minimum concentrations observed at STH_UB (0.22 μg m^{-3}). In summer, GRA_UB (0.34 μg m^{-3}) and ATH_UB (0.30 μg m^{-3}) exhibited the maximum contribution of eBC_{RC}. Seasonal patterns of eBC_T and eBC_{RC} were not homogenous across the studied sites, possibly due to variations in the emission and climate patterns in the different regions and cities.

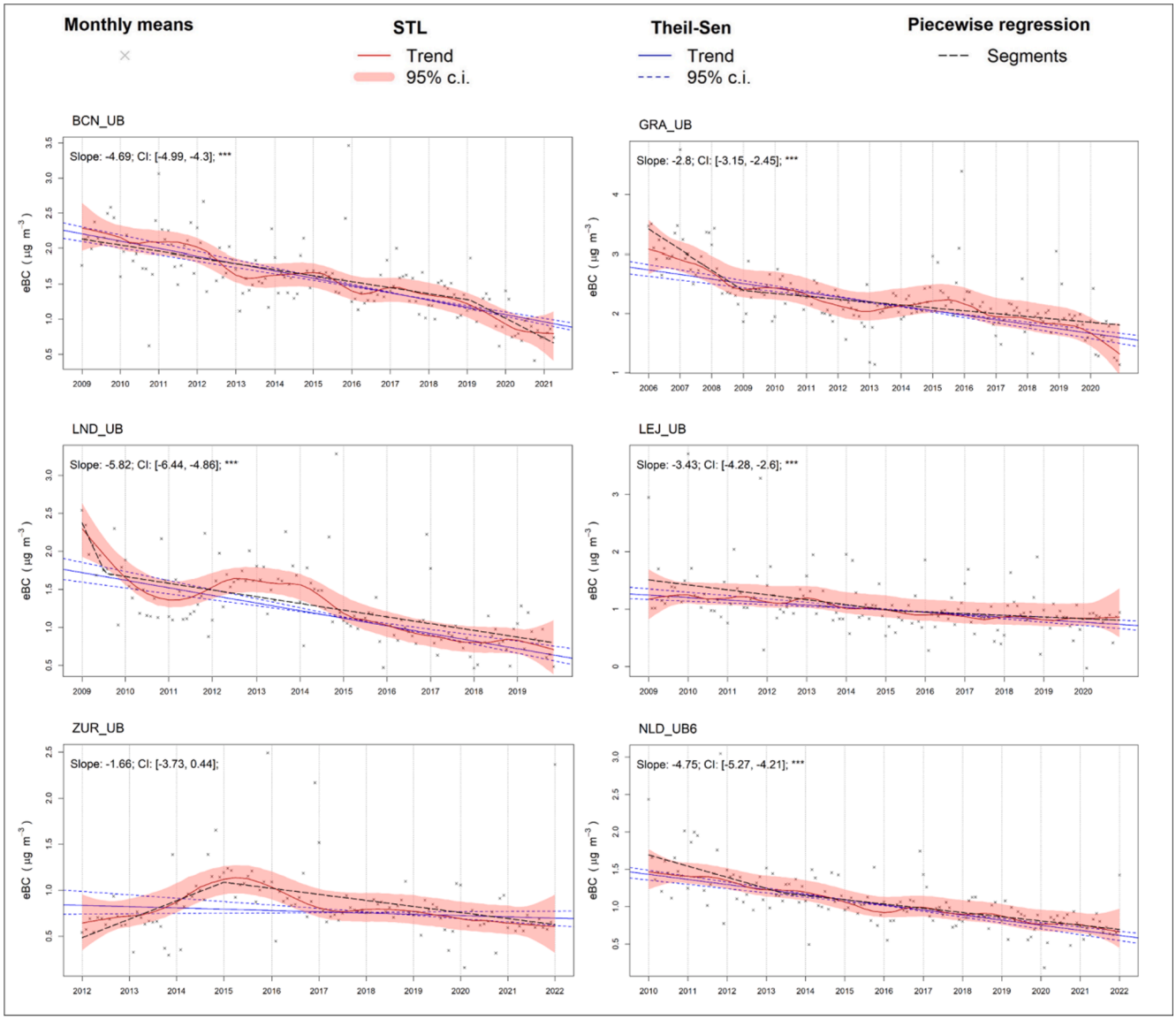

Fig. 8. Trends in eBC mass concentration for selected UB sites. The slope of the trends is given in % yr^{-1}. The statistically significant trends of each site are represented by *** for $p < 0.001$, ** for $p < 0.01$, * for $p < 0.05$, + for $p < 0.1$, and ns for not significant. The 95% confidence intervals (CI) for STL and MK-TS analyses were computed by bootstrapping.

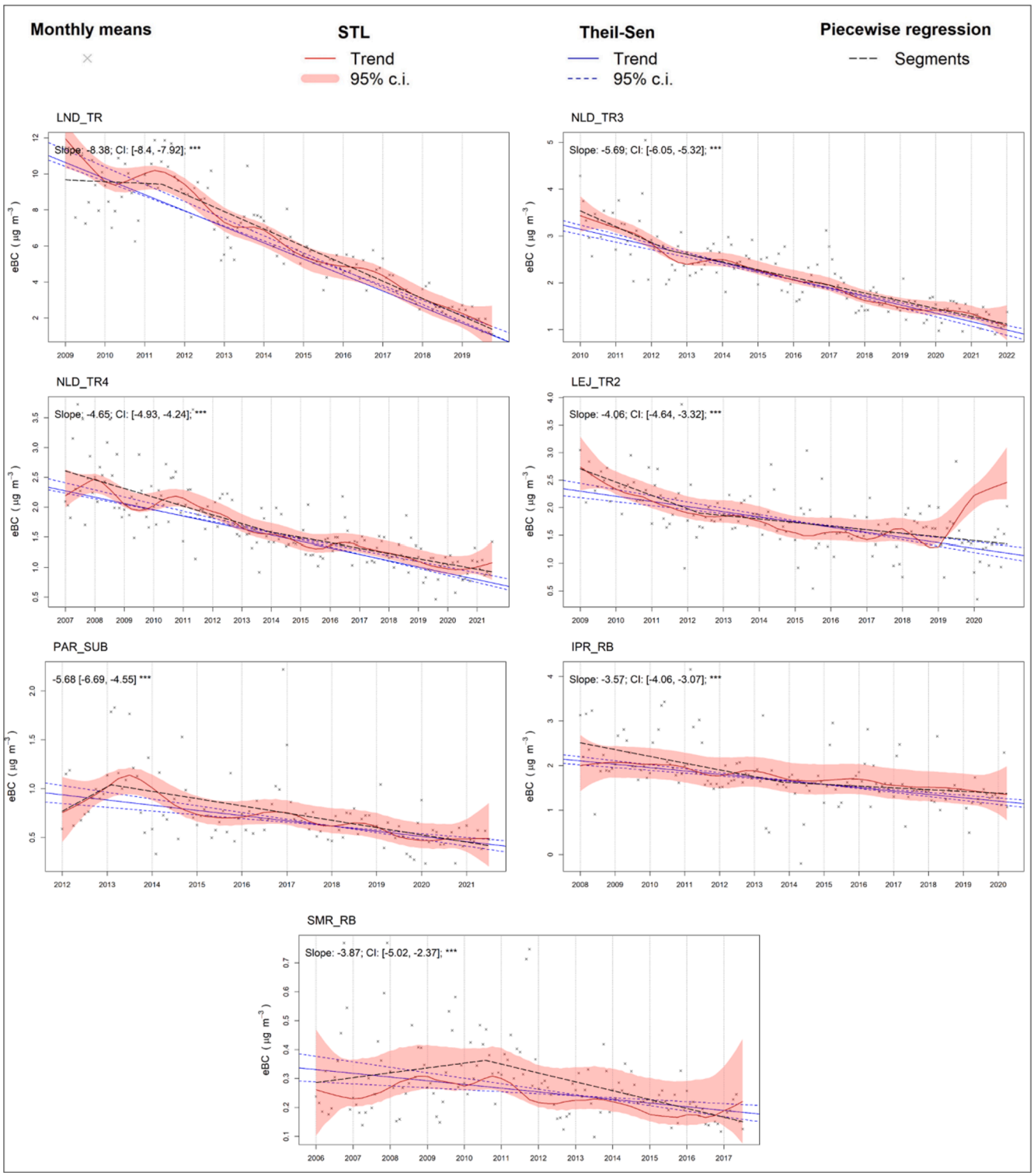

Fig. 9. Trends in eBC mass concentration for selected TR and RB sites. The slope of the trends is given in % yr-1. The statistically significant trends of each site are represented by *** for $p < 0.001$, ** for $p < 0.01$, * for $p < 0.05$, + for $p < 0.1$, and ns for not significant. The 95% confidence intervals (CI.) for STL and MK-TS analyses were computed by bootstrap.

3.4. Trend analysis

Figs. 8 and 9 represent the estimated inter-annual trends of eBC mass concentrations for selected sites with more than nine years of eBC observations between 2006 and 2020. The results of the Theil-Sen trend analysis, which include the slopes and corresponding confidence intervals, are presented in Fig. S6. This figure presents the standard errors of the breakpoints using the "segmented" R package, as well as the slopes and confidence intervals obtained from the Theil-Sen trend analysis. Annual deseasonalized STL trends and MK-TS, Theil-Sen slopes as well as the results of the piecewise linear regression computed throughout the year (annual) can be found in Table S5 and S6. Table S5 provides the corresponding *p*-values, slopes, and confidence intervals (CI). Table S6 provides details on the number of breakpoints, the dates of

identified breakpoints, standard errors, adjusted R^2 values (model accuracy), root mean squared errors (RMSEs), and mean absolute errors (MAEs) expressed in μg m^{-3}.

A consistent, statistically significant decreasing trend was detected at all sites during the observation period. This decreasing eBC trend is consistent with several European and American studies that have been conducted in recent years (Ahmed et al., 2014; Collaud Coen et al., 2020; Jafar and Harrison, 2021; Kutzner et al., 2018; Luoma et al., 2021; Masiol et al., 2018; Mousavi et al., 2018; Olstrup et al., 2018; Sun et al., 2021; Veld et al., 2021; Wang et al., 2014). These results are in contrast to previous studies conducted between 1960 and 2007, which reported an increase in eBC, especially in developing countries (Wang et al., 2014). In this study, the observed decreasing trends were associated with the European- and local-scale measures to improve AQ in urban areas. The observed trends in eBC mass concentrations can be influenced by different factors specific to each site over time, the details of which are beyond the scope of this paper. However, it is important to note that the enforcement of diesel filter traps since the EURO5 vehicle emission standards were enacted and the economic crisis in 2008 may have had a decisive contribution to these trends (Lyamani et al., 2011; Querol et al., 2014). A summary of the results obtained by applying three methods for the trend analyses is presented in Figs. 8 and 9.

In North-Western Europe, statistically significant decreasing trends were identified at both LND_TR and LND_UB sites between 2009 and 2019, with annual percentage decreases of –5.8% and –8.4% yr^{-1}, respectively. Our findings are consistent with the work published by Ciupek et al. (2021), who also reported a decreasing trend in eBC concentrations for LND_TR and LND_UB sites between 2014 and 2019, with decreases of up to –13%. These reductions have been attributed to the decline in PM emissions from diesel vehicles over the last decade, as well as an increase in the proportion of low-emission buses in London (Ciupek et al., 2021). The results of piecewise linear regression analysis confirmed that this strong drop had a detectable breakpoint in 2009 at LND_UB. A similar breakpoint was also observed at LND_TR in 2011. These findings are consistent with the trend analyses of eBC concentrations conducted in the UK between 2009 and 2016, particularly highlighting the substantial decrease in eBC of around –8 ± 3% per year observed at LND_TR (Singh et al., 2018). It should be noticed that the declining trend in LND_TR has been reported to be notable compared to other sites in UK (Singh et al., 2018). The findings of Singh et al. (2018) and Jafar and Harrison (2021) emphasize the fact that the reduced eBC levels at both London sites were due to the decrease in vehicle exhaust emissions and the effect of traffic emission abatement policies.

In Central Europe, the decreasing trends in eBC mass concentrations over time were more pronounced at German TR sites compared to UB sites. This trend is consistent with recent literature that found that trends at TR sites show larger declines in eBC concentrations over time compared to UB sites (Kutzner et al., 2018). Decreasing trends were observed at LEJ_UB and LEJ_TR sites in Central Europe, with annual percentage decreases of –3.4% yr^{-1} and –4.1% yr^{-1} respectively (see Figs. 8 and 9). These results are consistent with a recent study that demonstrated a decreasing trend in eBC over Central Europe between 2009 and 2018 (Sun et al., 2020, 2021). The introduction of low emission zones in Leipzig in 2011 has also led to substantial reductions in eBC mass concentrations, resulting in an 18–36% decrease between 2005 and 2014 (Kutzner et al., 2018; Rasch et al., 2013). Piecewise linear regression also revealed a strong drop with one breakpoint at LEJ_TR2 in 2012. However, STL and piecewise regressions did not identify any similar rapidly declining trends in eBC mass concentrations around the UB site. In addition, a decreasing trend of –3.5% yr^{-1} was observed at IPR_RB. Piecewise linear regression also revealed one breakpoint in 2014. According to the published report in 2018, emissions stemming from biomass burning for domestic heating and fossil fuel combustion related to transport and domestic heating around IPR_RB showed an increase of eBC_{RC}/eBC_T ratio during the years 2009–2010 that could potentially be linked to the economic crisis. Then remained relatively stable until 2013 (with a local minimum in 2011), and have generally exhibited a downward trend since that time (Putaud et al., 2018).

This study also revealed a statistically significant decreasing trend in eBC of –4.7% yr^{-1} between 2010 and 2020 at BCN_UB, consistent with a reported significant decrease (−18%) in eBC from 2014 to 2018 (Via et al., 2021). Piecewise linear regression and STL showed best fits with the Theil-Sen slope with one breakpoint in 2019. This suggests that the main driver of this decrease in mass concentrations may have been the implementation of traffic emission abatement policies (Carnerero et al., 2021). The GRA_UB site exhibits a slightly weaker decreasing trend, although it is still statistically significant (–2.8% yr^{-1}; see Fig. 8). The results of the STL and piecewise linear regression analysis are consistent with Theil-Sen, with one significant breakpoint detected in 2009, probably related with the economic recession experienced in 2008. This observation may also have been strongly affected by the implementation of EURO 4 and EURO 5 standards, which led to a reduction in emissions of PM and CO from both road traffic (resulting in a progressive downward trend) and industrial sources (resulting in sharp changes in 2007–2008) (Querol et al., 2014).

In central Europe, ZUR_UB exhibited a slightly decreasing (but not statistically significant) trend in 2012–2022 eBC mass concentrations at a rate of –1.7% yr^{-1}. This result is consistent with the results reported by Grange et al. (2020) at the same site, exhibiting a modestly decreasing trend in eBC_T at a rate of − 0.059 μg m^{-3} yr^{-1}. However, according to the same study, this trend is even lower or nearly constant for eBC_{RC} at ZUR_UB (–0.0062 μg m^{-3} yr^{-1}). The results of the piecewise linear regression revealed an increasing trend between 2012 and –2015, followed by a breakpoint in 2015, and then a declining trend from this point onward. This anomaly was also clearly observed by the STL method and can be attributed to a change in the aethalometer from an AE31 model to an AE33 model in April 2014 (Grange et al., 2020).

In Western and Northern Europe, similar statistically significant decreasing trends were observed at NLD_TR3, NLD_TR4, and NLD_UB6. These decreasing trends ranged between –4.6% yr^{-1} to –5.7% yr^{-1} between 2010 and 2020. Piecewise linear regression analysis at the Rotterdam sites showed the best fit with a slight but detectable breakpoint at NLD_TR3 in 2012. At the NLD_TR4 and NLD_UB6 sites, the declining trends were better estimated with one breakpoint in 2014 and 2013, respectively. This can be attributed to the implementation of stricter European emission standards for new road vehicles as well as a reduction in coal combustion for energy and heat production (Ruyssenaars et al., 2021).

The SMR_RB site showed a slightly lower (but still statistically significant) decreasing trend of –3.9% yr^{-1}, consistent with the decreasing trend in eBC reported by Luoma et al. (2021) for the same site. This decreasing trend was mostly driven by a sharp decrease in eBC concentrations after 2010, as detected by STL and piecewise linear regressions (see Fig. 9). The main reason for this change can be attributed to a Europe-wide decrease in eBC emissions (especially traffic) since a significant portion of eBC in SMR_RB originates from regional and long-range transported pollutants (Luoma et al., 2021). Meteorological parameters might also have played a role, due to the impact of weather changes on pollutant trends (i.e., unusually milder winters leading to a reduced need to burn wood for heating and the better mixing of pollutants in winter), which may be an indication of the impact of climate change in Europe (Borge et al., 2019; Peduzzi et al., 2020; Vetter et al., 2015).

In Western Europe, the PAR_SUB exhibits a statistically significant decreasing trend of –5.7% yr^{-1}, which is consistent with the reductions in NO_x, eBC_T, and hydrocarbon-like organic aerosol concentrations reported by Petit et al. (2021). This site is affected by road transport emissions and residential wood burning originating from PAR. The observed trends at the PAR_SUB site were affected by the implementation of mitigation policies as well as the decline of industrial activities in Western Europe (Zhang et al., 2018). Piecewise linear regression also

revealed an increasing trend with one breakpoint in 2013, which is likely associated with the replacement of the AE31 instrument with an AE33 model. However, all linear regression results computed after this breakpoint revealed a decreasing trend in eBC mass concentrations at PAR_SUB.

Despite the different periods considered, the decreasing trends in eBC reported in this study are consistent with the trends in particle absorption coefficients at a majority of European regional background sites as reported by Collaud Coen et al. (2020), who reported statistically significant decreasing trends in particles absorption ranging from around –0.4% yr^{-1} to –11.8% yr^{-1} over a ten-year period. In this study, which focused on urban sites, the statistically significant decreasing trends in eBC ranged from –1.6% yr^{-1} to –8.4% yr^{-1}.

In general, several studies have provided evidence supporting the similarities between the decreasing trend in eBC mass concentrations as well as those observed in NO_X and NO_2, which can mainly be attributed to a local reduction in traffic emission (Casquero-Vera et al., 2019; Olstrup et al., 2018). This pattern has been widely reported to be due to the implementation of emission mitigation policies in Europe, which have contributed to the decline in BC emissions (Sun et al., 2021). For instance, Henschel et al. 2016 reported that NO_x levels in European cities exhibited decreasing trends due to legislation aimed at controlling vehicle emissions. In addition, air pollution control plans have demonstrated positive impacts on improving AQ (Wen et al., 2020). The trends observed in eBC concentrations as well as the identified breakpoints in this study are consistent with annual BC emission inventories reported in Europe (European Monitoring and Evaluation Programme [EMEP], 2023), which considers primary pollutants from the road and off-road traffic, as well as other stationary combustion sources, including residential and commercial heating in major cities in their respective countries (see Fig. S5). Discrepancies in BC emission inventories can be influenced by factors such as the 2008 financial crisis in Europe, country-wide emission factors, source profiles, and activity levels that do not necessarily reflect local conditions. Additional sources of discrepancies can also be due to differences in open biomass burning (wildfires and agricultural waste) for which carbon emissions are highly variable (Chow et al., 2010).

In general, despite the demonstrated effect of the COVID-19 lockdown on the concentration levels of eBC across Europe (e.g., Evangeliou et al., 2021), the trends reported here do not show a clear impact of COVID-19. One possible reason could be the granularity of the time series data of the eBC trends reported in this work (the use of monthly averages) as well as the relatively rapid recovery in eBC emissions to rates similar to pre-lockdown conditions. However, Figs. 8 and 9 show that the decrease in monthly averages during the 2020 lockdown was more evident in the South of Europe (i.e. BCN_UB and GRA_UB) compared to Central and North Europe. This is consistent with the work on eBC emissions published by Evangeliou et al. (2021).

It is beyond the scope of this paper to explore the causes of the observed trends of eBC mass concentration in detail. This is primarily due to the difficulty of interpreting evolving trends over time. However, our detected breakpoints are mostly consistent with previous studies that have highlighted the importance of the implementation of diesel filter traps, which began in October 2009 in the EU. The diversity of the type, degree, and timing of local (urban) mitigation strategies in conjunction with the progressive abatement of emissions by EURO standards may also have shifted the breakpoints at each site.

Fig. 10 presents the long-term trends of eBC_T and eBC_{RC}

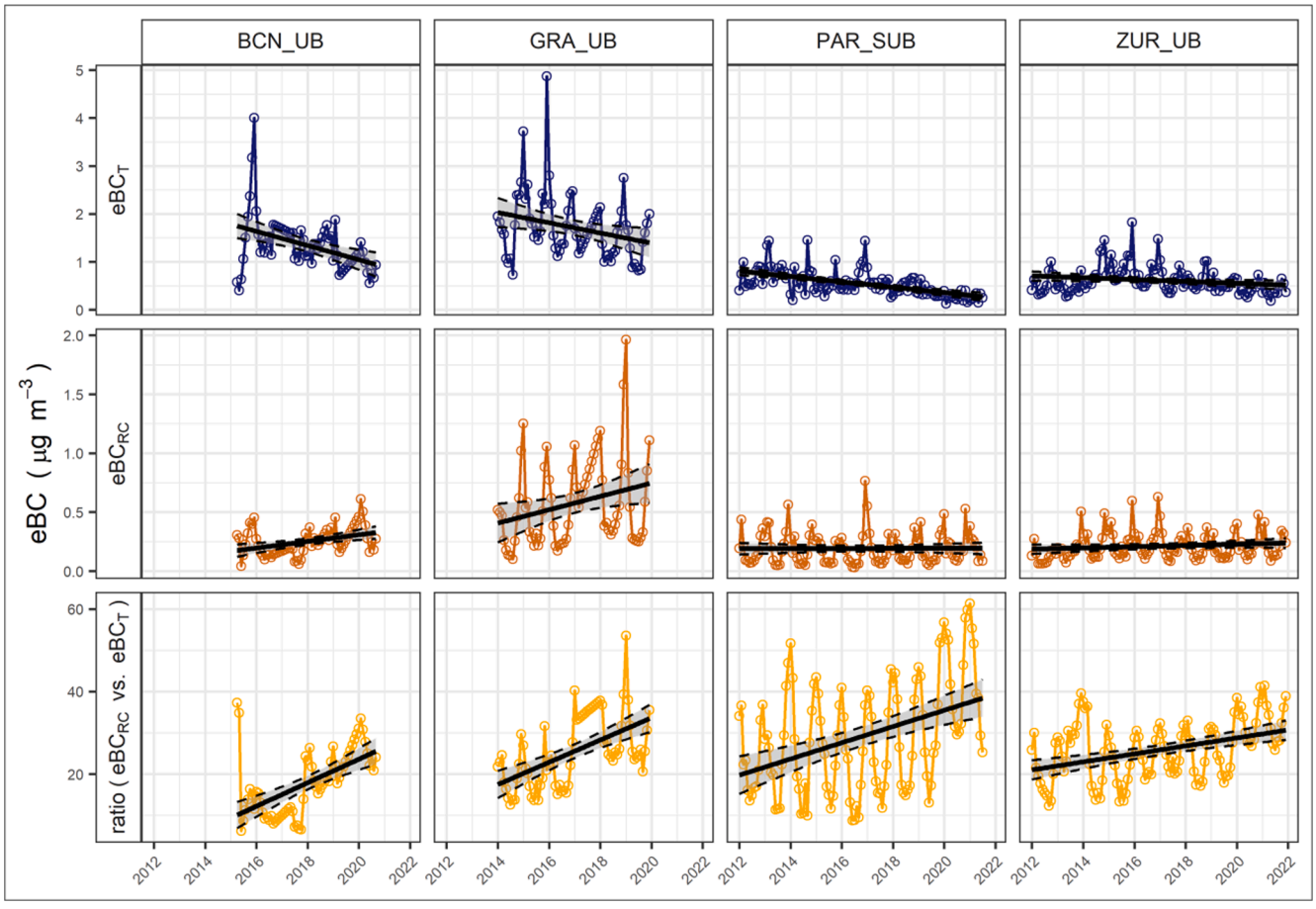

Fig. 10. Long-term trends in eBC_T and eBC_{RC}. The trends are reported as %-reduction or %-increase per year at the 95% confidence intervals of the fit as well as the eBC_{RC}/eBC_T ratio.

contributions. The data in Fig. 10 was produced by a linear least squares method due to its effectiveness in determining the optimal fit for a specific trend. In all examples, decreasing trends in eBC_T were statistically significant, while the relative contribution of eBC_{RC} remained fairly constant or had slightly increased, such as at GRA_UB and PAR_SUB. Decreasing trends in traffic and industrial PM and eBC emissions in developed countries as well as the promotion of biomass fuels for residential and commercial uses may have increased the relative contribution of solid fuels to eBC (Mousavi et al., 2018). Long-term studies on wood-burning trends in the UK have revealed that this source has the greatest variability in emissions, with larger eBC concentrations and PM contributions during cold months, although considerable decreasing trends have been observed between 2015 and 2021 (Font et al., 2022). Nevertheless, wood burning has been associated with increased public health risks due to increased PM levels in specific urban areas, particularly in Central European cities (Masiol et al., 2020; Tsiodra et al., 2021). Additional studies have also demonstrated that biomass burning has a significant impact on regional PM due to its widespread use (Cordell et al., 2016; Helin et al., 2018; Sandradewi et al., 2008a; Sandradewi et al., 2008b). Thus, the effects of biomass burning on AQ across Europe are of critical concern as it contributes to enhanced PM_{10}, and $PM_{2.5}$ mass concentrations (Cheng et al., 2022). In addition, trends in benzo(a)pyrene (BaP) and other carcinogenic polycyclic aromatic hydrocarbons (PAHs) associated with biomass burning have also exhibited similar behavior (Tsiodra et al., 2021). Similarly, long-term trends in eBC concentrations in the Northern US have also highlighted the importance of regional eBC sources from residential wood burning (Ahmed et al., 2014).

The trends in absolute eBC_T concentrations were most notable at the BCN_UB ($-0.14\ \mu g m^{-3}\ yr^{-1}$); eBC_T ranged from -0.02 to $-0.14\ \mu g\ m^{-3}\ yr^{-1}$ at BCN_UB, GRA_UB, PAR_SUB, and ZUR_UB as four case studies. The eBC_{RC} trends varied from 0.0 to 0.03 $\mu g\ m^{-3}\ yr^{-1}$ among the selected UB and SUB stations, showcasing a constant or slightly increasing trend. This is likely to have been driven by an increase in wood-burning emissions due to support from climate policies and the 2008 financial crisis (IPCC, 2019; WHO, World Health Organization, 2021). The approximately constant or increasing eBC_{RC} concentrations observed in this study period highlight the need for additional regulative measures to meet mandatory AQ standards, which will consequently minimize any adverse effects on human health.

4. Conclusions

This study provides a comprehensive overview of the concentrations, source apportionment, and spatial and temporal variability of ambient mass concentrations of eBC in UB, TR, and SUB environments in Europe. The datasets used in this analysis range from 2006 to 2022 and were collected using filter absorption photometer techniques. The study compiled and analyzed data from 50 sites, primarily located in urban areas across Europe. ACTRIS harmonization factors were used for different aethalometer types to standardize the calculation of the absorption coefficients. Only a low proportion of sites had co-located BC and EC measurements; accordingly, the MAC factor used to convert the measured absorptions into eBC mass concentrations was supplied by the instruments and was not obtained in situ.

This harmonized dataset revealed a marked decreasing trend in eBC mass concentrations as follows: TR > UB > SUB > RB, although there were some exceptions, such as the high eBC values observed at the RB site in the Po Valley (Northern Italy), a well-known hotspot in PM pollution. The average eBC mass concentrations ranged from 3.4 $\mu g\ m^{-3}$ at MLN_TR2 to 0.17 $\mu g\ m^{-3}$ at SMR_RB based on measurements from 2017 to 2019. There was also a noticeable decreasing trend in eBC concentrations at UB sites from southern to northern Europe. This north–south pattern is consistent with patterns observed for other pollutants, such as NO_2 or $PM_{2.5}$ mass concentration, and is attributed to variations in emissions and climate patterns across the studied region. The eBC mass concentrations observed in this study exhibited strong seasonal variability, with the highest observed values occurring during winter at MLN_TR2 ($5.2 \pm 2.8\ \mu g\ m^{-3}$), while the lowest values occurred in summer at SMR_RB ($0.1 \pm 0.1\ \mu g\ m^{-3}$).

The contributions of eBC_T and eBC_{RC} were estimated using an aethalometer source apportionment model between 2017 and 2019. The monthly-averaged contribution of eBC_T and eBC_{RC} revealed that the ratio of eBC_{RC}/eBC_T emissions increased during winter. The source apportionment analysis revealed that the sites with the highest relative eBC_T contributions were located in Western (PAR_UB) and Central (MLN_TR2) Europe, while the lowest contributions were observed in the Northern (HEL_SUB) and Eastern (BUC_SUB) regions. The relative contribution of eBC_{RC} was found to be higher at the BUC_SUB, ATH_UB, and HEL_SUB sites, highlighting the high relative eBC contributions from heating. As expected, the relative contributions and absolute concentrations of eBC_{RC} were higher during the cold seasons due to increased residential and commercial emissions as well as atmospheric stagnation. This study also clearly highlights the significant decreasing trend in eBC and eBC_T between 2006 and 2022 at both TR and UB sites in Europe, while the eBC_{RC} mass concentrations remained relatively constant or exhibited a slightly increasing trend in some locations. The decreasing trends in eBC mass concentration among all sites varied from $-1.6\%\ yr^{-1}$ to $-8.4\%\ yr^{-1}$. The absolute trends in eBC mass concentration were most notable at the TR sites, which varied from $-0.09\ \mu g\ m^{-3}\ yr^{-1}$ to $-0.9\ \mu g\ m^{-3}\ yr^{-1}$. At UB and RB stations, the absolute trends ranged from -0.02 to $-0.1\ \mu g\ m^{-3}\ yr^{-1}$ and -0.01 to $-0.07\ \mu g\ m^{-3}\ yr^{-1}$, respectively.

5. Recommendations and limitations

The World Health Organization has emphasized the importance of eBC measurements and their potential implications for public health (WHO, 2021). Furthermore, the proposed revision to the European Union Directive on AQ highlights the necessity of eBC measurements at both urban and regional background sites. This study has compiled eBC mass concentration data from 50 stations in (mostly urban) Europe, but the use of different methodological approaches for collecting eBC measurements poses challenges for the direct comparison of the collected data. This highlights the necessity of implementing harmonized methods, such as the ACTRIS procedures, to ensure consistency and facilitate meaningful comparisons. A major limitation of this study was the use of different instrumentation across the sites as well as potential instrument changes that may have occurred during the study period, which could have affected the comparability of time series data and trends. Furthermore, it is crucial to compile information on various parameters, including the filter tape characteristics (such as multiple-scattering parameter and leakage factor for AE instruments), inlet size-cut and length, the loading effect compensation algorithm, and measurement conditions (temperature, pressure, and humidity). It is important to note that the absolute BC concentration can also be influenced by the choice of the MAC factor. Indeed, MAC values can vary between different sites as well as over time depending on the physicochemical properties of eBC particles. Furthermore, the results of the aethalometer source apportionment model are dependent on the selected AAE values. Thus, the use of eBC as a relevant metric for AQ standards necessitates the use of harmonized measurement procedures and data processing methods. Accordingly, ACTRIS and future RI-URBANS studies should assess spatiotemporal variations in MAC to facilitate comparisons of eBC mass concentrations across urban Europe, determine appropriate approaches for the future reporting of eBC measurements, and provide recommendations for the selection of site-specific AAE values for source apportionment studies. It is important to note that the procedure used in this paper does not imply a recommendation from RI-URBANS or ACTRIS regarding the utilization of the instrument's default MAC values in all circumstances. For instance, using the average ACTRIS MAC value or site-specific MAC value

obtained through comparisons with co-located EC measurements where feasible may be part of the final recommendations proposed by RI-URBANS and ACTRIS for consolidated datasets.

Nevertheless, it is important to note that eBC monitoring can provide valuable insights into the effectiveness of AQ policies and standards. The results presented in this study demonstrate that concentrations of eBC originating from road traffic have significantly decreased over the past decade. However, eBC emissions from residential and commercial combustion sources have either remained constant or, in some cases, even increased. These trends primarily reflect the effective implementation of abatement strategies targeting traffic-related eBC emissions. Nevertheless, they also emphasize the necessity of implementing policies to mitigate other significant emissions sources, such as those from residential and commercial sectors. Further research should focus on evaluating the cause-effect response functions between eBC concentrations and health outcomes, specifically in cities where relevant health data is accessible to RI-URBANS.

CRediT authorship contribution statement

Marjan Savadkoohi: Data curation, Formal analysis, Investigation, Visualization, Writing – original draft, Writing – review & editing. **Marco Pandolfi:** Conceptualization, Methodology, Validation, Resources, Writing – review & editing, Supervision, Funding acquisition. **Cristina Reche:** Data curation. **Jarkko V. Niemi:** Data curation, Review. **Dennis Mooibroek:** Data curation, Review. **Gloria Titos:** Data curation, Review, Funding acquisition. **David C. Green:** Data curation, Funding acquisition. **Anja H. Tremper:** Data curation, Review, Funding acquisition. **Christoph Hueglin:** Data curation, Review. **Eleni Liakakou:** Data curation. **Nikos Mihalopoulos:** Data curation. **Iasonas Stavroulas:** Data curation. **Begoña Artiñano:** Data curation. **Esther Coz:** Data curation. **Lucas Alados-Arboledas:** Data curation, Funding acquisition. **David Beddows:** Data curation. **Véronique Riffault:** Data curation, Funding acquisition. **Joel F. De Brito:** Data curation, Funding acquisition. **Susanne Bastian:** Data curation. **Alexia Baudic:** Data curation. **Cristina Colombi:** Data curation. **Francesca Costabile:** Data curation, Funding acquisition. **Benjamin Chazeau:** Data curation. **Nicolas Marchand:** Data curation, Review. **José Luis Gómez-Amo:** Data curation, Funding acquisition. **Víctor Estellés:** Data curation. **Violeta Matos:** Data curation. **Ed van der Gaag:** Data curation. **Grégory Gille:** Data curation. **Krista Luoma:** Data curation. **Hanna E. Manninen:** Data curation. **Michael Norman:** Data curation, Funding acquisition. **Sanna Silvergren:** Data curation, Funding acquisition. **Jean-Eudes Petit:** Data curation, Review. **Jean-Philippe Putaud:** Data curation, Review. **Oliver V. Rattigan:** Data curation. **Hilkka Timonen:** Data curation. **Thomas Tuch:** Data curation. **Maik Merkel:** Data curation. **Kay Weinhold:** Data curation. **Stergios Vratolis:** Data curation. **Jeni Vasilescu:** Data curation, Funding acquisition. **Olivier Favez:** Data curation, Review & Editing. **Roy M. Harrison:** Data curation, Review & Editing. **Paolo Laj:** Review & Editing. **Alfred Wiedensohler:** Data curation, Review & Editing. **Philip K. Hopke:** Data curation, Review & Editing, Validation. **Tuukka Petäjä:** Data curation, Review & Editing, Validation. **Andrés Alastuey:** Conceptualization, Methodology, Validation, Resources, Writing – review & editing, Supervision, Funding acquisition. **Xavier Querol:** Conceptualization, Methodology, Validation, Resources, Writing – review & editing, Supervision, Funding acquisition.

Declaration of Competing Interest

The authors declare that they have no known competing financial interests or personal relationships that could have appeared to influence the work reported in this paper.

Data availability

The time series of eBC mass concentrations and absorption coefficients of 50 studied sites are available (DOI: https://doi.org/10.5281/zenodo.7982201).

Acknowledgments

This study is supported by the RI-URBANS project (Research Infrastructures Services Reinforcing Air Quality Monitoring Capacities in European Urban & Industrial Areas, European Union's Horizon 2020 research and innovation program, Green Deal, European Commission, contract 101036245). RI-URBANS is implementing the ACTRIS (https://actris.eu/) strategy for the development of services for improving air quality in Europe. The authors would like to also thank the support from "Agencia Estatal de Investigación" from the Spanish Ministry of Science and Innovation under the project CAIAC (PID2019-108990RB-I00) and the Generalitat de Catalunya (AGAUR, SGR-447) M. Savadkoohi would like to thank the Spanish Ministry of Science and Innovation for her FPI grant (PRE-2020-095498). This study is also part funded by the National Institute for Health Research (NIHR) Health Protection Research Unit in Environmental Exposures and Health, a partnership between UK Health Security Agency (UKHSA) and Imperial College London, and the UK Natural Environment Research Council. The views expressed are those of the author(s) and not necessarily those of the NIHR, UKHSA or the Department of Health and Social Care. The measurements in Stockholm (SE) were funded by the Swedish Environmental Protection Agency. The work performed in Rome (IT) was supported by ARPA Lazio, the regional Environmental Protection Agency.

This work was also carried out through the Core Program within the Romanian National Research Development and Innovation Plan 2022-2027, with the support of MCID, project no. PN 23 05 and through the European Regional Development Fund through the Competitiveness Operational Programme 2014–2020, Action 1.1.3 Creating synergies with H2020 Programme, project Strengthen the participation of the ACTRIS-RO consortium in the pan-European research infrastructure ACTRIS, ACTRIS-ROC, MYSMIS code 107596 (ctr. no.337/2021). Measurements at Granada urban station were possible thanks to the "Agencia Estatal de Investigación" from the Spanish Ministry of Science and Innovation under the projects PID2020-120015RB-I00 and PID2021-128757OB-I00, and ACTRIS-España (CGL2017-90884REDT). Measurements at Burjassot Atmospheric Station are supported by the Spanish Ministry of Economy and Competitiveness (MINECO) though the projects: RTI2018-096548-B-I00, PID2021-123881OB-I00 and TED2021-129185B-I00; and the Valencia Autonomous Government project: AICO/2021/341. IMT Nord Europe acknowledges financial support from the Labex CaPPA project, which is funded by the French National Research Agency (ANR) through the PIA (Programme d'Investissement d'Avenir) under contract ANR-11-LABX-0005-01, and the CLIMIBIO and ECRIN projects, both financed by the Regional Council "Hauts-de-France" and the European Regional Development Fund (ERDF). The ATOLL site is one of the French ACTRIS National Facilities and contributes to the CARA program of the LCSQA funded by the French Ministry of Environment.

Appendix A. Supplementary material

Supplementary data to this article can be found online at https://doi.org/10.1016/j.envint.2023.108081.

References

ACTRIS-ECAC. Recommendations, guidelines, satandard operating procedures and scientific articles for aerosol in-situ measurements. https://www.actris-ecac.eu/measurement-guidelines.html (accessed 8.31.22).

Ahmed, T., Dutkiewicz, V.A., Khan, A.J., Husain, L., 2014. Long term trends in Black Carbon Concentrations in the Northeastern United States. Atmos. Res. 137, 49–57. https://doi.org/10.1016/j.atmosres.2013.10.003.

Amato, F., Alastuey, A., Karanasiou, A., Lucarelli, F., Nava, S., Calzolai, G., Severi, M., Becagli, S., Gianelle, V.L., Colombi, C., Alves, C., Custódio, D., Nunes, T., Cerqueira, M., Pio, C., Eleftheriadis, K., Diapouli, E., Reche, C., Minguillón, M.C., Manousakas, M.I., Maggos, T., Vratolis, S., Harrison, R.M., Querol, X., 2016. AIRUSE-LIFE+: A harmonized PM speciation and source apportionment in five southern European cities. Atmos. Chem. Phys. 16, 3289–3309. https://doi.org/10.5194/acp-16-3289-2016.

Asmi, E., Backman, J., Servomaa, H., Virkkula, A., Gini, M.I., Eleftheriadis, K., Müller, T., Ohata, S., Kondo, Y., Hyvärinen, A., 2021. Absorption instruments inter-comparison campaign at the Arctic Pallas station. Atmos. Meas. Tech. 14, 5397–5413. https://doi.org/10.5194/amt-14-5397-2021.

Baldasano, J.M., 2020. COVID-19 lockdown effects on air quality by NO2 in the cities of Barcelona and Madrid (Spain). Sci. Total Environ. 741 https://doi.org/10.1016/j.scitotenv.2020.140353.

M. F. Barreira, L., Helin, A., Aurela, M., Teinila, K., Friman, M., Kangas, L., V. Niemi, J., Portin, H., Kousa, A., Pirjola, L., Ronkko, T., Saarikoski, S., Timonen, H., 2021. In-depth characterization of submicron particulate matter inter-annual variations at a street canyon site in northern Europe. Atmos. Chem. Phys. 21, 6297–6314. doi: 10.5194/acp-21-6297-2021.

Becerril-Valle, M., Coz, E., Prévôt, A.S.H., Močnik, G., Pandis, S.N., Sánchez de la Campa, A.M., Alastuey, A., Díaz, E., Pérez, R.M., Artíñano, B., 2017. Characterization of atmospheric black carbon and co-pollutants in urban and rural areas of Spain. Atmos. Environ. 169, 36–53. https://doi.org/10.1016/j.atmosenv.2017.09.014.

Blanco-Donado, E.P., Schneider, I.L., Artaxo, P., Lozano-Osorio, J., Portz, L., Oliveira, M. L.S., 2022. Source identification and global implications of black carbon. Geosci. Front. 13, 101149 https://doi.org/10.1016/j.gsf.2021.101149.

Bond, T.C., Doherty, S.J., Fahey, D.W., Forster, P.M., Berntsen, T., Deangelo, B.J., Flanner, M.G., Ghan, S., Kärcher, B., Koch, D., Kinne, S., Kondo, Y., Quinn, P.K., Sarofim, M.C., Schultz, M.G., Schulz, M., Venkataraman, C., Zhang, H., Zhang, S., Bellouin, N., Guttikunda, S.K., Hopke, P.K., Jacobson, M.Z., Kaiser, J.W., Klimont, Z., Lohmann, U., Schwarz, J.P., Shindell, D., Storelvmo, T., Warren, S.G., Zender, C.S., 2013. Bounding the role of black carbon in the climate system: A scientific assessment. J. Geophys. Res. Atmos. 118, 5380–5552. https://doi.org/10.1002/jgrd.50171.

Borge, R., Requia, W.J., Yagüe, C., Jhun, I., Koutrakis, P., 2019. Impact of weather changes on air quality and related mortality in Spain over a 25 year period [1993–2017]. Environ. Int. 133, 105272 https://doi.org/10.1016/j.envint.2019.105272.

Bressi, M., Cavalli, F., Putaud, J.P., Fröhlich, R., Petit, J.E., Aas, W., Äijälä, M., Alastuey, A., Allan, J.D., Aurela, M., Berico, M., Bougiatioti, A., Bukowiecki, N., Canonaco, F., Crenn, V., Dusanter, S., Ehn, M., Elsasser, M., Flentje, H., Graf, P., Green, D.C., Heikkinen, L., Hermann, H., Holzinger, R., Hueglin, C., Keernik, H., Kiendler-Scharr, A., Kubelová, L., Lunder, C., Maasikmets, M., Makeš, O., Malaguti, A., Mihalopoulos, N., Nicolas, J.B., O'Dowd, C., Ovadnevaite, J., Petralia, E., Poulain, L., Priestman, M., Riffault, V., Ripoll, A., Schlag, P., Schwarz, J., Sciare, J., Slowik, J., Sosedova, Y., Stavroulas, I., Teinemaa, E., Via, M., Vodička, P., Williams, P.I., Wiedensohler, A., Young, D.E., Zhang, S., Favez, O., Minguillón, M.C., Prevot, A.S.H., 2021. A European aerosol phenomenology - 7: High-time resolution chemical characteristics of submicron particulate matter across Europe. Atmos. Environ. X 10. https://doi.org/10.1016/j.aeaoa.2021.100108.

Briggs, N.L., Long, C.M., 2016. Critical review of black carbon and elemental carbon source apportionment in Europe and the United States. Atmos. Environ. 144, 409–427. https://doi.org/10.1016/j.atmosenv.2016.09.002.

Carnerero, C., Rivas, I., Reche, C., Pérez, N., Alastuey, A., Querol, X., 2021. Trends in primary and secondary particle number concentrations in urban and regional environments in NE Spain. Atmos. Environ. 244 https://doi.org/10.1016/j.atmosenv.2020.117982.

Carslaw, D.C., Ropkins, K., 2012. Openair - An r package for air quality data analysis. Environ. Model. Softw. 27–28, 52–61. https://doi.org/10.1016/j.envsoft.2011.09.008.

Casquero-Vera, J.A., Lyamani, H., Titos, G., Borrás, E., Olmo, F.J., Alados-Arboledas, L., 2019. Impact of primary NO2 emissions at different urban sites exceeding the European NO2 standard limit. Sci. Total Environ. 646, 1117–1125. https://doi.org/10.1016/j.scitotenv.2018.07.360.

Cassee, F.R., Morawska, L., Peters, A., Wierzbicka, A., Buonanno, G., Cyrys, J., SchnelleKreis, J., Kowalski, M., Riediker, M., Birmili, W., Querol, X., Yildirim, A.Ö., Elder, A., Yu, I.J., Øvrevik, J., Hougaard, K.S., Loft, S., Schmid, O., Schwarze, P.E., Stöger, T., Schneider, A., Okokon, E., Samoli, E., Stafoggia, M., Pickford, R., Zhang, S., Breitner, S., Schikowski, T., Lanki, T., Tobias, A., 2019. Ambient ultrafine particles: evidence for policy makers [White paper] 1–23.

Cavalli, F., Alastuey, A., Areskoug, H., Ceburnis, D., Čech, J., Genberg, J., Harrison, R.M., Jaffrezo, J.L., Kiss, G., Laj, P., Mihalopoulos, N., Perez, N., Quincey, P., Schwarz, J., Sellegri, K., Spindler, G., Swietlicki, E., Theodosi, C., Yttri, K.E., Aas, W., Putaud, J. P., 2016. A European aerosol phenomenology -4: Harmonized concentrations of carbonaceous aerosol at 10 regional background sites across Europe. Atmos. Environ. 144, 133–145. https://doi.org/10.1016/j.atmosenv.2016.07.050.

Chazeau, B., El Haddad, I., Canonaco, F., Temime-Roussel, B., D'Anna, B., Gille, G., Mesbah, B., Prévôt, A.S.H., Wortham, H., Marchand, N., 2022. Organic aerosol source apportionment by using rolling positive matrix factorization: Application to a Mediterranean coastal city. Atmos. Environ. X 14. https://doi.org/10.1016/j.aeaoa.2022.100176.

Chebaicheb, H., Brito, J.F. De, Chen, G., Tison, E., Favez, O., Marchand, C., Pr, S.H., 2023. Investigation of four-year chemical composition and organic aerosol sources of submicron particles at the ATOLL site in northern France ☆ 330. doi: 10.1016/j.envpol.2023.121805.

Chen, G., Canonaco, F., Tobler, A., Aas, W., Alastuey, A., Allan, J., Atabakhsh, S., Aurela, M., Baltensperger, U., Bougiatioti, A., De Brito, J.F., Ceburnis, D., Chazeau, B., Chebaicheb, H., Daellenbach, K.R., Ehn, M., El Haddad, I., Eleftheriadis, K., Favez, O., Flentje, H., Font, A., Fossum, K., Freney, E., Gini, M., Green, D.C., Heikkinen, L., Herrmann, H., Kalogridis, A.C., Keernik, H., Lhotka, R., Lin, C., Lunder, C., Maasikmets, M., Manousakas, M.I., Marchand, N., Marin, C., Marmureanu, L., Mihalopoulos, N., Močnik, G., Nęcki, J., O'Dowd, C., Ovadnevaite, J., Peter, T., Petit, J.E., Pikridas, M., Matthew Platt, S., Pokorná, P., Poulain, L., Priestman, M., Riffault, V., Rinaldi, M., Różański, K., Schwarz, J., Sciare, J., Simon, L., Skiba, A., Slowik, J.G., Sosedova, Y., Stavroulas, I., Styszko, K., Teinemaa, E., Timonen, H., Tremper, A., Vasilescu, J., Via, M., Vodička, P., Wiedensohler, A., Zografou, O., Cruz Minguillón, M., Prévôt, A.S.H., 2022. European aerosol phenomenology – 8: Harmonised source apportionment of organic aerosol using 22 Year-long ACSM/AMS datasets. Environ. Int. 166 https://doi.org/10.1016/j.envint.2022.107325.

Cheng, Y.H., Huang, Y.C., Pipal, A.S., Jian, M.Y., Liu, Z.S., 2022. Source apportionment of black carbon using light absorption measurement and impact of biomass burning smoke on air quality over rural central Taiwan: A yearlong study. Atmos. Pollut. Res. 13, 101264 https://doi.org/10.1016/j.apr.2021.101264.

Cho, C., Kim, S.W., Lee, M., Lim, S., Fang, W., Gustafsson, Ö., Andersson, A., Park, R.J., Sheridan, P.J., 2019. Observation-based estimates of the mass absorption cross-section of black and brown carbon and their contribution to aerosol light absorption in East Asia. Atmos. Environ. 212, 65–74. https://doi.org/10.1016/j.atmosenv.2019.05.024.

Chow, J.C., Watson, J.G., Lowenthal, D.H., Chen, L.W.A., Motallebi, N., 2010. Black and organic carbon emission inventories: Review and application to California. J. Air Waste Manag. Assoc. 60, 497–507. https://doi.org/10.3155/1047-3289.60.4.497.

Ciupek, K., Quincey, P., Green, D.C., Butterfield, D., Fuller, G.W., 2021. Challenges and policy implications of long-term changes in mass absorption cross-section derived from equivalent black carbon and elemental carbon measurements in London and south-east England in 2014–2019. Environ. Sci. Process. Impacts 23, 1949–1960. https://doi.org/10.1039/d1em00200g.

Cleveland, Robert B., Cleveland, William S., McRea, Jean E., Terpenning, I., 1990. STL A Seasonal-Trend Decomposition Procedure Based on Loess (with Discussion).

Collaud Coen, M., Andrews, E., Lastuey, A., Petkov Arsov, T., Backman, J., Brem, B.T., Bukowiecki, N., Couret, C., Eleftheriadis, K., Flentje, H., Fiebig, M., Gysel-Beer, M., Hand, J.L., Hoffer, A., Hooda, R., Hueglin, C., Joubert, W., Keywood, M., Eun Kim, J., Kim, S.W., Labuschagne, C., Lin, N.H., Lin, Y., Lund Myhre, C., Luoma, K., Lyamani, H., Marinoni, A., Mayol-Bracero, O.L., Mihalopoulos, N., Pandolfi, M., Prats, N., Prenni, A.J., Putaud, J.P., Ries, L., Reisen, F., Sellegri, K., Sharma, S., Sheridan, P., Patrick Sherman, J., Sun, J., Titos, G., Torres, E., Tuch, T., Weller, R., Wiedensohler, A., Zieger, P., Laj, P., 2020. Multidecadal trend analysis of in situ aerosol radiative properties around the world. Atmos. Chem. Phys. 20, 8867–8908. https://doi.org/10.5194/acp-20-8867-2020.

Cordell, R.L., Mazet, M., Dechoux, C., Hama, S.M.L., Staelens, J., Hofman, J., Stroobants, C., Roekens, E., Kos, G.P.A., Weijers, E.P., Frumau, K.F.A., Panteliadis, P., Delaunay, T., Wyche, K.P., Monks, P.S., 2016. Evaluation of biomass burning across North West Europe and its impact on air quality. Atmos. Environ. 141, 276–286. https://doi.org/10.1016/j.atmosenv.2016.06.065.

Crilley, L.R., Bloss, W.J., Yin, J., Beddows, D.C.S., Harrison, R.M., Allan, J.D., Young, D. E., Flynn, M., Williams, P., Zotter, P., Prevot, A.S.H., Heal, M.R., Barlow, J.F., Halios, C.H., Lee, J.D., Szidat, S., Mohr, C., 2015. Sources and contributions of wood smoke during winter in London: Assessing local and regional influences. Atmos. Chem. Phys. 15, 3149–3171. https://doi.org/10.5194/acp-15-3149-2015.

Crippa, M., Decarlo, P.F., Slowik, J.G., Mohr, C., Heringa, M.F., Chirico, R., Poulain, L., Freutel, F., Sciare, J., Cozic, J., Di Marco, C.F., Elsasser, M., Nicolas, J.B., Marchand, N., Abidi, E., Wiedensohler, A., Drewnick, F., Schneider, J., Borrmann, S., Nemitz, E., Zimmermann, R., Jaffrezo, J.L., Prévôt, A.S.H., Baltensperger, U., 2013. Wintertime aerosol chemical composition and source apportionment of the organic fraction in the metropolitan area of Paris. Atmos. Chem. Phys. 13, 961–981. https://doi.org/10.5194/acp-13-961-2013.

Cuesta-Mosquera, A., Mocnik, G., Drinovec, L., Müller, T., Pfeifer, S., Minguillon, M.C., Briel, B., Buckley, P., Dudoitis, V., Fernández-García, J., Fernandez-Amado, M., De Brito, J.F., Riffault, V., Flentje, H., Heffernan, E., Kalivitis, N., Kalogridis, A.C., Keernik, H., Marmureanu, L., Luoma, K., Marinoni, A., Pikridas, M., Schauer, G., Serfozo, N., Servomaa, H., Titos, G., Yus-Diez, J., Zioła, N., Wiedensohler, A., 2021. Intercomparison and characterization of 23 Aethalometers under laboratory and ambient air conditions: Procedures and unit-to-unit variabilities. Atmos. Meas. Tech. 14, 3195–3216. https://doi.org/10.5194/amt-14-3195-2021.

Diapouli, E., Kalogridis, A.C., Markantonaki, C., Vratolis, S., Fetfatzis, P., Colombi, C., Eleftheriadis, K., 2017. Annual variability of black carbon concentrations originating from biomass and fossil fuel combustion for the suburban aerosol in Athens, Greece. Atmosphere (Basel). 8 https://doi.org/10.3390/atmos8120234.

Drinovec, L., Močnik, G., Zotter, P., Prévôt, A.S.H., Ruckstuhl, C., Coz, E., Rupakheti, M., Sciare, J., Müller, T., Wiedensohler, A., Hansen, A.D.A., 2015. The "dual-spot" Aethalometer: An improved measurement of aerosol black carbon with real-time loading compensation. Atmos. Meas. Tech. 8, 1965–1979. https://doi.org/10.5194/amt-8-1965-2015.

EBAS, Atmospheric measurement data. https://ebas-data.nilu.no/ (accessed 9.13.22).

EEA, European Environment Agency. Classification of monitoring stations and criteria to include them in EEA's assessments products. https://www.eea.europa.eu/th

emes/air/air-quality-concentrations/classification-of-monitoring-stations-and (accessed 2.6.23).
El Haddad, I., D'Anna, B., Temime-Roussel, B., Nicolas, M., Boreave, A., Favez, O., Voisin, D., Sciare, J., George, C., Jaffrezo, J.L., Wortham, H., Marchand, N., 2013. Towards a better understanding of the origins, chemical composition and aging of oxygenated organic aerosols: Case study of a Mediterranean industrialized environment, Marseille. Atmos. Chem. Phys. 13, 7875–7894. https://doi.org/10.5194/acp-13-7875-2013.
EMEP, Centre on Emission Inventories and Projections. Data viewer - officially reported emissions data. https://www.ceip.at/data-viewer (accessed 1.30.23).
Evangeliou, N., Platt, S.M., Eckhardt, S., Lund Myhre, C., Laj, P., Alados-Arboledas, L., Backman, J., Brem, B.T., Fiebig, M., Flentje, H., Marinoni, A., Pandolfi, M., Yus-Dìez, J., Prats, N., Putaud, J.P., Sellegri, K., Sorribas, M., Eleftheriadis, K., Vratolis, S., Wiedensohler, A., Stohl, A., 2021. Changes in black carbon emissions over Europe due to COVID-19 lockdowns. Atmos. Chem. Phys. 21, 2675–2692. https://doi.org/10.5194/acp-21-2675-2021.
Favez, O., Cachier, H., Sciare, J., Sarda-Estève, R., Martinon, L., 2009. Evidence for a significant contribution of wood burning aerosols to PM2.5 during the winter season in Paris. France. Atmos. Environ. 43, 3640–3644. https://doi.org/10.1016/j.atmosenv.2009.04.035.
Favez, O., El Haddad, I., Piot, C., Boréave, A., Abidi, E., Marchand, N., Jaffrezo, J.L., Besombes, J.L., Personnaz, M.B., Sciare, J., Wortham, H., George, C., D'Anna, B., 2010. Inter-comparison of source apportionment models for the estimation of wood burning aerosols during wintertime in an Alpine city (Grenoble, France). Atmos. Chem. Phys. 10, 5295–5314. https://doi.org/10.5194/acp-10-5295-2010.
Font, A., Ciupek, K., Butterfield, D., Fuller, G.W., 2022. Long-term trends in particulate matter from wood burning in the United Kingdom: Dependence on weather and social factors. Environ. Pollut. 314, 120105 https://doi.org/10.1016/j.envpol.2022.120105.
Fung, P.L., Sillanpää, S., Niemi, J.V., Kousa, A., Timonen, H., Zaidan, M.A., Saukko, E., Kulmala, M., Petäjä, T., Hussein, T., 2022. Improving the current air quality index with new particulate indicators using a robust statistical approach. Sci. Total Environ. 844 https://doi.org/10.1016/j.scitotenv.2022.157099.
Garg, S., Chandra, B.P., Sinha, V., Sarda-Esteve, R., Gros, V., Sinha, B., 2016. Limitation of the Use of the Absorption Angstrom Exponent for Source Apportionment of Equivalent Black Carbon: A Case Study from the North West Indo-Gangetic Plain. Environ. Sci. Technol. 50, 814–824. https://doi.org/10.1021/acs.est.5b03868.
Geels, C., Winther, M., Andersson, C., Jalkanen, J.P., Brandt, J., Frohn, L.M., Im, U., Leung, W., Christensen, J.H., 2021. Projections of shipping emissions and the related impact on air pollution and human health in the Nordic region. Atmos. Chem. Phys. 21, 12495–12519. https://doi.org/10.5194/acp-21-12495-2021.
Geng, F., Hua, J., Mu, Z., Peng, L., Xu, X., Chen, R., Kan, H., 2013. Differentiating the associations of black carbon and fine particle with daily mortality in a Chinese city. Environ. Res. 120, 27–32. https://doi.org/10.1016/j.envres.2012.08.007.
Gilardoni, S., Massoli, P., Marinoni, A., Mazzoleni, C., Freedman, A., Lonati, G., De Iuliis, S., Gianelle, V., 2020. Spatial and temporal variability of carbonaceous aerosol absorption in the Po Valley. Aerosol Air Qual. Res. 20, 2624–2639. https://doi.org/10.4209/aaqr.2020.03.0085.
Grange, S.K., Fischer, A., Zellweger, C., Alastuey, A., Querol, X., Jaffrezo, J.L., Weber, S., Uzu, G., Hueglin, C., 2021. Switzerland's PM10 and PM2.5 environmental increments show the importance of non-exhaust emissions. Atmos. Environ. X 12 https://doi.org/10.1016/j.aeaoa.2021.100145.
Grange, S., Lötscher, H., Fischer, A., Emmenegger, L., Hueglin, C., 2020. Evaluation of equivalent black carbon source apportionment using observations from Switzerland between 2008 and 2018. Atmos. Meas. Tech. 13, 1867–1885. https://doi.org/10.5194/amt-13-1867-2020.
Grivas, G., Stavroulas, I., Liakakou, E., Kaskaoutis, D.G., Bougiatioti, A., Paraskevopoulou, D., Gerasopoulos, E., Mihalopoulos, N., 2019. Measuring the spatial variability of black carbon in Athens during wintertime. Air Qual. Atmos. Heal. 12, 1405–1417. https://doi.org/10.1007/s11869-019-00756-y.
Harrison, R.M., Beddows, D.C.S., Jones, A.M., Calvo, A., Alves, C., Pio, C., 2013. An evaluation of some issues regarding the use of aethalometers to measure woodsmoke concentrations. Atmos. Environ. 80, 540–548. https://doi.org/10.1016/j.atmosenv.2013.08.026.
Helin, A., Niemi, J.V., Virkkula, A., Pirjola, L., Teinilä, K., Backman, J., Aurela, M., Saarikoski, S., Rönkkö, T., Asmi, E., Timonen, H., 2018. Characteristics and source apportionment of black carbon in the Helsinki metropolitan area, Finland. Atmos. Environ. 190, 87–98. https://doi.org/10.1016/j.atmosenv.2018.07.022.
Helin, A., Virkkula, A., Backman, J., Pirjola, L., Sippula, O., Aakko-Saksa, P., Väätäinen, S., Mylläri, F., Järvinen, A., Bloss, M., Aurela, M., Jakobi, G., Karjalainen, P., Zimmermann, R., Jokiniemi, J., Saarikoski, S., Tissari, J., Rönkkö, T., Niemi, J.V., Timonen, H., 2021. Variation of Absorption Ångström Exponent in Aerosols From Different Emission Sources. J. Geophys. Res. Atmos. 126, 1–21. https://doi.org/10.1029/2020JD034094.
Henschel, S., Le Tertre, A., Atkinson, R.W., Querol, X., Pandolfi, M., Zeka, A., Haluza, D., Analitis, A., Katsouyanni, K., Bouland, C., Pascal, M., Medina, S., Goodman, P.G., 2016. Trends of nitrogen oxides in ambient air in nine European cities between 1999 and 2010. Atmos. Environ. 117, 234–241. https://doi.org/10.1016/j.atmosenv.2015.07.013.
Herich, H., Hueglin, C., Buchmann, B., 2011. A 2.5 year's source apportionment study of black carbon from wood burning and fossil fuel combustion at urban and rural sites in Switzerland. Atmos. Meas. Tech. 4, 1409–1420. https://doi.org/10.5194/amt-4-1409-2011.
Hienola, A.I., Pietikäinen, J.P., Jacob, D., Pozdun, R., Petäjä, T., Hyvärinen, A.P., Sogacheva, L., Kerminen, V.M., Kulmala, M., Laaksonen, A., 2013. Black carbon concentration and deposition estimations in Finland by the regional aerosol-climate model REMO-HAM. Atmos. Chem. Phys. 13, 4033–4055. https://doi.org/10.5194/acp-13-4033-2013.
Hopke, P.K., Feng, Y., Dai, Q., 2022. Source apportionment of particle number concentrations: A global review. Sci. Total Environ. 819, 153104 https://doi.org/10.1016/j.scitotenv.2022.153104.
Hyvärinen, A.P., Kolmonen, P., Kerminen, V.M., Virkkula, A., Leskinen, A., Komppula, M., Hatakka, J., Burkhart, J., Stohl, A., Aalto, P., Kulmala, M., Lehtinen, K.E.J., Viisanen, Y., Lihavainen, H., 2011. Aerosol black carbon at five background measurement sites over Finland, a gateway to the Arctic. Atmos. Environ. 45, 4042–4050. https://doi.org/10.1016/j.atmosenv.2011.04.026.
Invernizzi, G., Ruprecht, A., Mazza, R., De Marco, C., Močnik, G., Sioutas, C., Westerdahl, D., 2011. Measurement of black carbon concentration as an indicator of air quality benefits of traffic restriction policies within the ecopass zone in Milan, Italy. Atmos. Environ. 45, 3522–3527. https://doi.org/10.1016/j.atmosenv.2011.04.008.
IPCC, Intergovernmental Panel on Climate Change, 2019. Global warming of 1.5°C, Special Report on Global Warming of 1.5°C. Intergovernmental Panel on Climate Change. https://www.ipcc.ch/sr15/ (accessed 2.6.23).
IPCC, Intergovernmental Panel on Climate Change, 2021. Climate Change 2021 - The Physical Science Basis - Summary for Policymakers, Climate Change 2021: The Physical Science Basis. doi:10.1017/9781009157896 (accessed 2.6.23).
Irwin, M., Kondo, Y., Moteki, N., 2015. An empirical correction factor for filter-based photo-absorption black carbon measurements. J. Aerosol Sci. 80, 86–97. https://doi.org/10.1016/j.jaerosci.2014.11.001.
Ivančič, M., Gregorič, A., Lavrič, G., Alföldy, B., Ježek, I., Hasheminassab, S., Pakbin, P., Ahangar, F., Sowlat, M., Boddeker, S., Rigler, M., 2022. Two-year-long high-time-resolution apportionment of primary and secondary carbonaceous aerosols in the Los Angeles Basin using an advanced total carbon–black carbon (TC-BC(λ)) method. Sci. Total Environ. 848 https://doi.org/10.1016/j.scitotenv.2022.157606.
Jafar, H.A., Harrison, R.M., 2021. Spatial and temporal trends in carbonaceous aerosols in the United Kingdom. Atmos. Pollut. Res. 12, 295–305. https://doi.org/10.1016/j.apr.2020.09.009.
Janssen, N.A.H., Hoek, G., Simic-Lawson, M., Fischer, P., van Bree, L., Brink, H.T., Keuken, M., Atkinson, R.W., Ross Anderson, H., Brunekreef, B., Cassee, F.R., 2011. Black carbon as an additional indicator of the adverse health effects of airborne particles compared with pm10 and pm2.5. Environ. Health Perspect. 119, 1691–1699. https://doi.org/10.1289/ehp.1003369.
Jing, A., Zhu, B., Wang, H., Yu, X., 2019. Source apportionment of black carbon in different seasons in the northern suburb of Nanjing. China. Atmos. Environ. 201, 190–200. https://doi.org/10.1016/j.atmosenv.2018.12.060.
Karagulian, F., Belis, C.A., Dora, C.F.C., Prüss-Ustün, A.M., Bonjour, S., Adair-Rohani, H., Amann, M., 2015. Contributions to cities' ambient particulate matter (PM): A systematic review of local source contributions at global level. Atmos. Environ. 120, 475–483. https://doi.org/10.1016/j.atmosenv.2015.08.087.
Kaskaoutis, D.G., Grivas, G., Stavroulas, I., Bougiatioti, A., Liakakou, E., Dumka, U.C., Gerasopoulos, E., Mihalopoulos, N., 2021. Apportionment of black and brown carbon spectral absorption sources in the urban environment of Athens, Greece, during winter. Sci. Total Environ. 801, 149739 https://doi.org/10.1016/j.scitotenv.2021.149739.
Keuken, M., Roemer, M., van den Elshout, S., 2009. Trend analysis of urban NO2 concentrations and the importance of direct NO2 emissions versus ozone/NOx equilibrium. Atmos. Environ. 43, 4780–4783. https://doi.org/10.1016/j.atmosenv.2008.07.043.
Knox, A., Evans, G.J., Brook, J.R., Yao, X., Jeong, C.H., Godri, K.J., Sabaliauskas, K., Slowik, J.G., 2009. Mass absorption cross-section of ambient black carbon aerosol in relation to chemical age. Aerosol Sci. Technol. 43, 522–532. https://doi.org/10.1080/02786820902777207.
Kondo, Y., Sahu, L., Kuwata, M., Miyazaki, Y., Takegawa, N., Moteki, N., Imaru, J., Han, S., Nakayama, T., Oanh, N.T.K., Hu, M., Kim, Y.J., Kita, K., 2009. Stabilization of the mass absorption cross section of black carbon for filter-based absorption photometry by the use of a heated inlet. Aerosol Sci. Technol. 43, 741–756. https://doi.org/10.1080/02786820902889879.
Krecl, P., Targino, A.C., Johansson, C., 2011. Spatiotemporal distribution of light-absorbing carbon and its relationship to other atmospheric pollutants in Stockholm. Atmos. Chem. Phys. 11, 11553–11567. https://doi.org/10.5194/acp-11-11553-2011.
Krecl, P., Johansson, C., Targino, A.C., Ström, J., Burman, L., 2017. Trends in black carbon and size-resolved particle number concentrations and vehicle emission factors under real-world conditions. Atmos. Environ. 165, 155–168. https://doi.org/10.1016/j.atmosenv.2017.06.036.
Kumar, S., Wang, S., Lin, N., Chantara, S., Lee, C., Thepnuan, D., 2020. Black carbon over an urban atmosphere in northern peninsular Southeast Asia : Characteristics, source apportionment, and associated health risks. Environ. Pollut. 259, 113871 https://doi.org/10.1016/j.envpol.2019.113871.
Kutzner, R.D., von Schneidemesser, E., Kuik, F., Quedenau, J., Weatherhead, E.C., Schmale, J., 2018. Long-term monitoring of black carbon across Germany. Atmos. Environ. 185, 41–52. https://doi.org/10.1016/j.atmosenv.2018.04.039.
Laborde, M., Crippa, M., Tritscher, T., Jurányi, Z., Decarlo, P.F., Temime-Roussel, B., Marchand, N., Eckhardt, S., Stohl, A., Baltensperger, U., Prévôt, A.S.H., Weingartner, E., Gysel, M., 2013. Black carbon physical properties and mixing state in the European megacity Paris. Atmos. Chem. Phys. 13, 5831–5856. https://doi.org/10.5194/acp-13-5831-2013.
Lack, D.A., Cappa, C.D., 2010. Impact of brown and clear carbon on light absorption enhancement, single scatter albedo and absorption wavelength dependence of black carbon. Atmos. Chem. Phys. 10, 4207–4220. https://doi.org/10.5194/acp-10-4207-2010.

Lack, D.A., Corbett, J.J., 2012. Black carbon from ships: A review of the effects of ship speed, fuel quality and exhaust gas scrubbing. Atmos. Chem. Phys. 12, 3985–4000. https://doi.org/10.5194/acp-12-3985-2012.

Laj, P., Bigi, A., Rose, C., Andrews, E., Lund Myhre, C., Collaud Coen, M., Lin, Y., Wiedensohler, A., Schulz, M., A. Ogren, J., Fiebig, M., Gliß, J., Mortier, A., Pandolfi, M., Petäja, T., Kim, S.W., Aas, W., Putaud, J.P., Mayol-Bracero, O., Keywood, M., Labrador, L., Aalto, P., Ahlberg, E., Alados Arboledas, L., Alastuey, A., Andrade, M., Artinano, B., Ausmeel, S., Arsov, T., Asmi, E., Backman, J., Baltensperger, U., Bastian, S., Bath, O., Paul Beukes, J., T. Brem, B., Bukowiecki, N., Conil, S., Couret, C., Day, D., Dayantolis, W., Degorska, A., Eleftheriadis, K., Fetfatzis, P., Favez, O., Flentje, H., I. Gini, M., Gregorič, A., Gysel-Beer, M., Gannet Hallar, A., Hand, J., Hoffer, A., Hueglin, C., K. Hooda, R., Hyvärinen, A., Kalapov, I., Kalivitis, N., Kasper-Giebl, A., Eun Kim, J., Kouvarakis, G., Kranjc, I., Krejci, R., Kulmala, M., Labuschagne, C., Lee, H.J., Lihavainen, H., Lin, N.H., Löschau, G., Luoma, K., Marinoni, A., Martins Dos Santos, S., Meinhardt, F., Merkel, M., Metzger, J.M., Mihalopoulos, N., Anh Nguyen, N., Ondracek, J., Pérez, N., Rita Perrone, M., Pichon, J.M., Picard, D., Pichon, J.M., Pont, V., Prats, N., Prenni, A., Reisen, F., Romano, S., Sellegri, K., Sharma, S., Schauer, G., Sheridan, P., Patrick Sherman, J., Schütze, M., Schwerin, A., Sohmer, R., Sorribas, M., Steinbacher, M., Sun, J., Titos, G., Toczko, B., Tuch, T., Tulet, P., Tunved, P., Vakkari, V., Velarde, F., Velasquez, P., Villani, P., Vratolis, S., Wang, S.H., Weinhold, K., Weller, R., Yela, M., Yus-Diez, J., Zdimal, V., Zieger, P., Zikova, N., 2020. A global analysis of climate-relevant aerosol properties retrieved from the network of Global Atmosphere Watch (GAW) near-surface observatories. Atmos. Meas. Tech. 13, 4353–4392. doi:10.5194/amt-13-4353-2020.

Li, J., Liu, C., Yin, Y., Kumar, K.R., 2016. Numerical investigation on the Ångström exponent of black carbon aerosol. J. Geophys. Res. Atmos. 121, 3506–3518. https://doi.org/10.1002/2015jd024718.

Liakakou, E., Stavroulas, I., Kaskaoutis, D.G., Grivas, G., Paraskevopoulou, D., Dumka, U. C., Tsagkaraki, M., Bougiatioti, A., Oikonomou, K., Sciare, J., Gerasopoulos, E., Mihalopoulos, N., 2020. Long-term variability, source apportionment and spectral properties of black carbon at an urban background site in Athens. Greece. Atmos. Environ. 222, 117137 https://doi.org/10.1016/j.atmosenv.2019.117137.

Liu, C., Chung, C.E., Yin, Y., Schnaiter, M., 2018. The absorption Ångström exponent of black carbon: From numerical aspects. Atmos. Chem. Phys. 18, 6259–6273. https://doi.org/10.5194/acp-18-6259-2018.

Luoma, K., Niemi, J.V., Aurela, M., Lun Fung, P., Helin, A., Hussein, T., Kangas, L., Kousa, A., Rönkkö, T., Timonen, H., Virkkula, A., Petäjä, T., 2021. Spatiotemporal variation and trends in equivalent black carbon in the Helsinki metropolitan area in Finland. Atmos. Chem. Phys. 21, 1173–1189. https://doi.org/10.5194/acp-21-1173-2021.

Lyamani, H., Olmo, F.J., Foyo, I., Alados-Arboledas, L., 2011. Black carbon aerosols over an urban area in south-eastern Spain: Changes detected after the 2008 economic crisis. Atmos. Environ. 45, 6423–6432. https://doi.org/10.1016/j.atmosenv.2011.07.063.

Martinsson, J., Abdul Azeem, H., Sporre, M.K., Bergström, R., Ahlberg, E., Öström, E., Kristensson, A., Swietlicki, E., Eriksson Stenström, K., 2017. Carbonaceous aerosol source apportionment using the Aethalometer model-evaluation by radiocarbon and levoglucosan analysis at a rural background site in southern Sweden. Atmos. Chem. Phys. 17, 4265–4281. https://doi.org/10.5194/acp-17-4265-2017.

Masiol, M., Squizzato, S., Chalupa, D.C., Utell, M.J., Rich, D.Q., Hopke, P.K., 2018. Long-term trends in submicron particle concentrations in a metropolitan area of the northeastern United States. Sci. Total Environ. 633, 59–70. https://doi.org/10.1016/j.scitotenv.2018.03.151.

Masiol, M., Squizzato, S., Formenton, G., Khan, M.B., Hopke, P.K., Nenes, A., Pandis, S. N., Tositti, L., Benetello, F., Visin, F., Pavoni, B., 2020. Hybrid multiple-site mass closure and source apportionment of PM2.5 and aerosol acidity at major cities in the Po Valley. Sci. Total Environ. 704, 135287 https://doi.org/10.1016/j.scitotenv.2019.135287.

Mbengue, S., Serfozo, N., Schwarz, J., Holoubek, I., Ziková, N., Šmejkalová, A.H., Holoubek, I., 2020. Characterization of Equivalent Black Carbon at a regional background site in Central Europe: Variability and source apportionment☆. Environ. Pollut. 260 https://doi.org/10.1016/j.envpol.2019.113771.

Mbengue, S., Zikova, N., Schwarz, J., Vodička, P., Šmejkalová, A.H., Holoubek, I., 2021. Mass absorption cross-section and absorption enhancement from long term black and elemental carbon measurements: A rural background station in Central Europe. Sci. Total Environ. 794 https://doi.org/10.1016/j.scitotenv.2021.148365.

Merabet, H., Kerbachi, R., Mihalopoulos, N., Stavroulas, I., Kanakidou, M., Yassaa, N., 2019. Measurement of atmospheric black carbon in some south mediterranean cities: Seasonal variations and source apportionment. Clean Air J. 29, 1–19. https://doi.org/10.17159/caj/2019/29/2.7500.

Milinković, A., Gregorič, A., Grgičin, V.D., Vidič, S., Penezić, A., Kušan, A.C., Alempijević, S.B., Kasper-Giebl, A., Frka, S., 2021. Variability of black carbon aerosol concentrations and sources at a Mediterranean coastal region. Atmos. Pollut. Res. 12 https://doi.org/10.1016/j.apr.2021.101221.

Minderytė, A., Pauraite, J., Dudoitis, V., Plauškaitė, K., Kilikevičius, A., Matijošius, J., Rimkus, A., Kilikevičienė, K., Vainorius, D., Byčenkienė, S., 2022. Carbonaceous aerosol source apportionment and assessment of transport-related pollution. Atmos. Environ. 279 https://doi.org/10.1016/j.atmosenv.2022.119043.

Moosmüller, H., Chakrabarty, R.K., Arnott, W.P., 2009. Aerosol light absorption and its measurement: A review. J. Quant. Spectrosc. Radiat. Transf. 110, 844–878. https://doi.org/10.1016/j.jqsrt.2009.02.035.

Mousavi, A., Sowlat, M.H., Hasheminassab, S., Polidori, A., Sioutas, C., 2018. Spatio-temporal trends and source apportionment of fossil fuel and biomass burning black carbon (BC) in the Los Angeles Basin. Sci. Total Environ. 640–641, 1231–1240. https://doi.org/10.1016/j.scitotenv.2018.06.022.

Mousavi, A., Sowlat, M.H., Lovett, C., Rauber, M., Szidat, S., Bo, R., Borgini, A., Marco, C. D., Ruprecht, A.A., Sioutas, C., Boffi, R., Borgini, A., De Marco, C., Ruprecht, A.A., Sioutas, C., Bo, R., Borgini, A., Marco, C.D., Ruprecht, A.A., Sioutas, C., 2019. Source apportionment of black carbon (BC) from fossil fuel and biomass burning in metropolitan Milan. Italy. Atmos. Environ. 203, 252–261. https://doi.org/10.1016/j.atmosenv.2019.02.009.

Muggeo, V.M.R., 2003. Estimating regression models with unknown break-points. Stat. Med. 22, 3055–3071. https://doi.org/10.1002/sim.1545.

Muggeo, V.M.R, 2008. segmented: an R Package to Fit Regression Models with Broken-Line Relationships. R news 8, 20–25. https://journal.r-project.org/articles/RN-2008-004/RN-2008-004.pdf (accessed 2.6.23).

Müller, T., Fiebig, M., 2018a. ACTRIS In Situ Aerosol: Guidelines for Manual QC of AE33 absorption photometer data. https://www.actris-ecac.eu/ (accessed 2.6.23).

Müller, T., Fiebig, M., 2018b. ACTRIS In Situ Aerosol: Guidelines for Manual QC of MAAP (Multiangle Absorption Photometer) data. https://www.actris-ecac.eu/ (accessed 2.6.23).

Müller, T., Henzing, J.S., De Leeuw, G., Wiedensohler, A., Alastuey, A., Angelov, H., Bizjak, M., Collaud Coen, M., Engström, J.E., Gruening, C., Hillamo, R., Hoffer, A., Imre, K., Ivanow, P., Jennings, G., Sun, J.Y., Kalivitis, N., Karlsson, H., Komppula, M., Laj, P., Li, S.M., Lunder, C., Marinoni, A., Martins Dos Santos, S., Moerman, M., Nowak, A., Ogren, J.A., Petzold, A., Pichon, J.M., Rodriquez, S., Sharma, S., Sheridan, P.J., Teinilä, K., Tuch, T., Viana, M., Virkkula, A., Weingartner, E., Wilhelm, R., Wang, Y.Q., 2011. Characterization and intercomparison of aerosol absorption photometers: Result of two intercomparison workshops. Atmos. Meas. Tech. 4, 245–268. https://doi.org/10.5194/amt-4-245-2011.

Olstrup, H., Forsberg, B., Orru, H., Nguyen, H., Molnár, P., Johansson, C., 2018. Trends in air pollutants and health impacts in three Swedish cities over the past three decades. Atmos. Chem. Phys. 18, 15705–15723. https://doi.org/10.5194/acp-18-15705-2018.

Pandolfi, M., Alados-arboledas, L., Alastuey, A., Andrade, M., Angelov, C., 2018. A European aerosol phenomenology – 6 : scattering properties of atmospheric aerosol particles from 28 ACTRIS sites 7877–7911. doi:10.5194/acp-18-7877-2018.

Pandolfi, M., Ripoll, A., Querol, X., Alastuey, A., 2014. Climatology of aerosol optical properties and black carbon mass absorption cross section at a remote high-altitude site in the western Mediterranean Basin. Atmos. Chem. Phys. 14, 6443–6460. https://doi.org/10.5194/acp-14-6443-2014.

Peduzzi, E., Baldi, M.G., Pisoni, E., Kona, A., Bertoldi, P., Monforti-Ferrario, F., 2020. Impacts of a climate change initiative on air pollutant emissions: Insights from the Covenant of Mayors. Environ. Int. 145, 106029 https://doi.org/10.1016/j.envint.2020.106029.

Petit, J.E., Dupont, J.C., Favez, O., Gros, V., Zhang, Y., Sciare, J., Simon, L., Truong, F., Bonnaire, N., Amodeo, T., Vautard, R., Haeffelin, M., 2021. Response of atmospheric composition to COVID-19 lockdown measures during spring in the Paris region (France). Atmos. Chem. Phys. 21, 17167–17183. https://doi.org/10.5194/acp-21-17167-2021.

Petzold, A., Schloesser, H., Sheridan, P.J., Arnott, W.P., Ogren, J.A., Virkkula, A., 2005. Evaluation of multiangle absorption photometry for measuring aerosol light absorption. Aerosol Sci. Technol. 39, 40–51. https://doi.org/10.1080/027868290901945.

Petzold, A., Ogren, J.A., Fiebig, M., Laj, P., Li, S.M., Baltensperger, U., Holzer-Popp, T., Kinne, S., Pappalardo, G., Sugimoto, N., Wehrli, C., Wiedensohler, A., Zhang, X.Y., 2013. Recommendations for reporting black carbon measurements. Atmos. Chem. Phys. 13, 8365–8379. https://doi.org/10.5194/acp-13-8365-2013.

Petzold, A., Schönlinner, M., 2004. Multi-angle absorption photometry - A new method for the measurement of aerosol light absorption and atmospheric black carbon. J. Aerosol Sci. 35, 421–441. https://doi.org/10.1016/j.jaerosci.2003.09.005.

Putaud, J.P., Cavalli, F., and Crippa, M., Long-term trends in black carbon from biomass and fossil fuel combustion detected at the JRC atmospheric observatory in Ispra., EUR 29147 EN, Publications Office of the European Union, Luxembourg, 2018, ISBN 978-92-79-80976-7, doi:10.2760/5944, JRC110502.

Putaud, J.P., Raes, F., Van Dingenen, R., Brüggemann, E., Facchini, M.C., Decesari, S., Fuzzi, S., Gehrig, R., Hüglin, C., Laj, P., Lorbeer, G., Maenhaut, W., Mihalopoulos, N., Müller, K., Querol, X., Rodriguez, S., Schneider, J., Spindler, G., Ten Brink, H., Tørseth, K., Wiedensohler, A., 2004. A European aerosol phenomenology - 2: Chemical characteristics of particulate matter at kerbside, urban, rural and background sites in Europe. Atmos. Environ. 38, 2579–2595. https://doi.org/10.1016/j.atmosenv.2004.01.041.

Putaud, J.P., Van Dingenen, R., Alastuey, A., Bauer, H., Birmili, W., Cyrys, J., Flentje, H., Fuzzi, S., Gehrig, R., Hansson, H.C., Harrison, R.M., Herrmann, H., Hitzenberger, R., Hüglin, C., Jones, A.M., Kasper-Giebl, A., Kiss, G., Kousa, A., Kuhlbusch, T.A.J., Löschau, G., Maenhaut, W., Molnar, A., Moreno, T., Pekkanen, J., Perrino, C., Pitz, M., Puxbaum, H., Querol, X., Rodriguez, S., Salma, I., Schwarz, J., Smolik, J., Schneider, J., Spindler, G., ten Brink, H., Tursic, J., Viana, M., Wiedensohler, A., Raes, F., 2010. A European aerosol phenomenology - 3: Physical and chemical characteristics of particulate matter from 60 rural, urban, and kerbside sites across Europe. Atmos. Environ. 44, 1308–1320. https://doi.org/10.1016/j.atmosenv.2009.12.011.

Querol, X., Alastuey, A., Pandolfi, M., Reche, C., Pérez, N., Minguillón, M.C., Moreno, T., Viana, M., Escudero, M., Orio, A., Pallarés, M., Reina, F., 2014. 2001–2012 trends on air quality in Spain. Sci. Total Environ. 490, 957–969. https://doi.org/10.1016/j.scitotenv.2014.05.074.

Rasch, F., Birmili, W., Weinhold, K., Nordmann, S., Sonntag, A., Spindler, G., Herrmann, H., Wiedensohler, A., Löschau, G., 2013. Significant reduction of ambient black carbon and particle number in Leipzig as a result of the low emission zone 73, Issue, 483–489.

Rigler, M., Drinovec, L., Lavri, G., Vlachou, A., Prevot, A.S.H., Luc Jaffrezo, J., Stavroulas, I., Sciare, J., Burger, J., Kranjc, I., Turšič, J., Hansen, D.A., A., Mocnik, G., 2020. The new instrument using a TC-BC (total carbon-black carbon) method for the online measurement of carbonaceous aerosols. Atmos. Meas. Tech. 13, 4333–4351. https://doi.org/10.5194/amt-13-4333-2020.

Ripoll, A., Minguillón, M.C., Pey, J., Jimenez, J.L., Day, D.A., Sosedova, Y., Canonaco, F., Prévôt, A.S.H., Querol, X., Alastuey, A., 2015. Long-term real-time chemical characterization of submicron aerosols at Montsec (southern Pyrenees, 1570 m a.s. l.). Atmos. Chem. Phys. 15, 2935–2951. https://doi.org/10.5194/acp-15-2935-2015.

RI-URBANS, 2020. Research Infrastructures Services Reinforcing Air Quality Monitoring Capacities in European Urban & Industrial AreaS (RI-URBANS), Technical annex, Horizon 2020, LC-GD-9-1-2020, Work programme H2020-2018-2020. https://riurbans.eu/.

Rivas, I., Beddows, D.C.S., Amato, F., Green, D.C., Järvi, L., Hueglin, C., Reche, C., Timonen, H., Fuller, G.W., Niemi, J.V., Pérez, N., Aurela, M., Hopke, P.K., Alastuey, A., Kulmala, M., Harrison, R.M., Querol, X., Kelly, F.J., 2020. Source apportionment of particle number size distribution in urban background and traffic stations in four European cities. Environ. Int. 135, 105345 https://doi.org/10.1016/j.envint.2019.105345.

Rivas, I., Vicens, L., Basagaña, X., Tobías, A., Katsouyanni, K., Walton, H., Hüglin, C., Alastuey, A., Kulmala, M., Harrison, R.M., Pekkanen, J., Querol, X., Sunyer, J., Kelly, F.J., 2021. Associations between sources of particle number and mortality in four European cities. Environ. Int. 155 https://doi.org/10.1016/j.envint.2021.106662.

Ruyssenaars, P.G., Coenen, P.W.H.G., Rienstra, J.D., Zijlema, P.J., Arets, E.J.M.M., Baas, K., Dröge, R., Geilenkirchen, G., 't Hoen, M., Honig, E., van Huet, B., van Huis, E.P., Koch, W.W.R., te Molder, R.M., Montfoort, J.A., van der Zee, T., van Zanten, M.C., 2021. Greenhouse gas emissions in the Netherlands 1990-2018, RIVM 2021, National Institute for Public Health and the Environment (RIVM). doi:10.21945/RIVM-2021-0007 P.G.

Salameh, D., Pey, J., Bozzetti, C., El Haddad, I., Detournay, A., Sylvestre, A., Canonaco, F., Armengaud, A., Piga, D., Robin, D., Prevot, A.S.H., Jaffrezo, J.L., Wortham, H., Marchand, N., 2018. Sources of PM2.5 at an urban-industrial Mediterranean city, Marseille (France): Application of the ME-2 solver to inorganic and organic markers. Atmos. Res. 214, 263–274. https://doi.org/10.1016/j.atmosres.2018.08.005.

Sandradewi, J., Prévôt, A.S.H., Szidat, S., Perron, N., Alfarra, M.R., Lanz, V.A., Weingartner, E., Baltensperger, U.R.S., 2008a. Using aerosol light abosrption measurements for the quantitative determination of wood burning and traffic emission contribution to particulate matter. Environ. Sci. Technol. 42, 3316–3323. https://doi.org/10.1021/es702253m.

Sandradewi, J., Prévôt, A.S.H., Weingartner, E., Schmidhauser, R., Gysel, M., Baltensperger, U., 2008b. A study of wood burning and traffic aerosols in an Alpine valley using a multi-wavelength Aethalometer. Atmos. Environ. 42, 101–112. https://doi.org/10.1016/j.atmosenv.2007.09.034.

Sandrini, S., Fuzzi, S., Piazzalunga, A., Prati, P., Bonasoni, P., Cavalli, F., Bove, M.C., Calvello, M., Cappelletti, D., Colombi, C., Contini, D., de Gennaro, G., Di Gilio, A., Fermo, P., Ferrero, L., Gianelle, V., Giugliano, M., Ielpo, P., Lonati, G., Marinoni, A., Massabò, D., Molteni, U., Moroni, B., Pavese, G., Perrino, C., Perrone, M.R.G., Perrone, M.R.G., Putaud, J.P., Sargolini, T., Vecchi, R., Gilardoni, S., 2014. Spatial and seasonal variability of carbonaceous aerosol across Italy. Atmos. Environ. 99, 587–598. https://doi.org/10.1016/j.atmosenv.2014.10.032.

Schaap, M., Denier van der Gon, H.A.C., 2007. On the variability of Black Smoke and carbonaceous aerosols in the Netherlands. Atmos. Environ. 41, 5908–5920. https://doi.org/10.1016/j.atmosenv.2007.03.042.

Segersson, D., Eneroth, K., Gidhagen, L., Johansson, C., Omstedt, G., Nylén, A.E., Forsberg, B., 2017. Health impact of PM10, PM2.5 and black carbon exposure due to different source sectors in Stockholm, Gothenburg and Umea, Sweden. Int. J. Environ. Res. Public Health 14, 11–14. https://doi.org/10.3390/ijerph14070742.

Segura, S., Estellés, V., Esteve, A.R., Marcos, C.R., Utrillas, M.P., Martínez-Lozano, J.A., 2016. Multiyear in-situ measurements of atmospheric aerosol absorption properties at an urban coastal site in western Mediterranean. Atmos. Environ. 129, 18–26. https://doi.org/10.1016/j.atmosenv.2016.01.008.

Singh, V., Ravindra, K., Sahu, L., Sokhi, R., 2018. Trends of atmospheric black carbon concentration over United Kingdom. Atmos. Environ. 178, 148–157. https://doi.org/10.1016/j.atmosenv.2018.01.030.

Srivastava, P., Naja, M., Seshadri, T.R., Joshi, H., Dumka, U.C., Gogoi, M.M., Babu, S.S., 2022. Implications of Site-specific Mass Absorption Cross-section (MAC) to Black Carbon Observations at a High-altitude Site in the Central Himalaya. Asia-Pacific J. Atmos. Sci. 58, 83–96. https://doi.org/10.1007/s13143-021-00241-6.

Sun, J., Birmili, W., Hermann, M., Tuch, T., Weinhold, K., Merkel, M., Rasch, F., Müller, T., Schladitz, A., Bastian, S., Löschau, G., Cyrys, J., Gu, J., Flentje, H., Briel, B., Asbach, C., Kaminski, H., Ries, L., Sohmer, R., Gerwig, H., Wirtz, K., Meinhardt, F., Schwerin, A., Bath, O., Ma, N., Wiedensohler, A., 2020. Decreasing trends of particle number and black carbon mass concentrations at 16 observational sites in Germany from 2009 to 2018. Atmos. Chem. Phys. 20, 7049–7068. https://doi.org/10.5194/acp-20-7049-2020.

Sun, J., Hermann, M., Yuan, Y., Birmili, W., Coen, M.C., Weinhold, K., Madueño, L., Poulain, L., Tuch, T., Ries, L., Sohmer, R., Couret, C., Frank, G., Brem, B.T., Beer, M. G., Ma, N., Wiedensohler, A., 2021. Long - term trends of black carbon and particle number concentration in the lower free troposphere in Central Europe. Environ. Sci. Eur. doi:10.1186/s12302-021-00488-w.

Titos, G., del Águila, A., Cazorla, A., Lyamani, H., Casquero-Vera, J.A., Colombi, C., Cuccia, E., Gianelle, V., Močnik, G., Alastuey, A., Olmo, F.J., Alados-Arboledas, L., 2017. Spatial and temporal variability of carbonaceous aerosols: Assessing the impact of biomass burning in the urban environment. Sci. Total Environ. 578, 613–625. https://doi.org/10.1016/j.scitotenv.2016.11.007.

Tobler, A.K., Skiba, A., Canonaco, F., Močnik, G., Rai, P., Chen, G., Bartyzel, J., Zimnoch, M., Styszko, K., Nęcki, J., Furger, M., Rózański, K., Baltensperger, U., Slowik, J.G., Prevot, A.S.H., 2021. Characterization of non-refractory (NR) PM1and source apportionment of organic aerosol in Kraków. Poland. Atmos. Chem. Phys. 21, 14893–14906. https://doi.org/10.5194/acp-21-14893-2021.

Tsiodra, I., Grivas, G., Tavernaraki, K., Bougiatioti, A., Apostolaki, M., Paraskevopoulou, D., Gogou, A., Parinos, C., Oikonomou, K., Tsagkaraki, M., Zarmpas, P., Nenes, A., Mihalopoulos, N., 2021. Annual exposure to polycyclic aromatic hydrocarbons in urban environments linked to wintertime wood-burning episodes. Atmos. Chem. Phys. 21, 17865–17883. https://doi.org/10.5194/acp-21-17865-2021.

UK AIR, Department for Environment Food & Rural Affairs. Site environment types-Defra, UK. https://uk-air.defra.gov.uk/networks/site-types (accessed 8.31.22).

Van Dingenen, R., Raes, F., Putaud, J.P., Baltensperger, U., Charron, A., Facchini, M.C., Decesari, S., Fuzzi, S., Gehrig, R., Hansson, H.C., Harrison, R.M., Hüglin, C., Jones, A.M., Laj, P., Lorbeer, G., Maenhaut, W., Palmgren, F., Querol, X., Rodriguez, S., Schneider, J., Ten Brink, H., Tunved, P., Tørseth, K., Wehner, B., Weingartner, E., Wiedensohler, A., Wåhlin, P., 2004. A European aerosol phenomenology - 1: Physical characteristics of particulate matter at kerbside, urban, rural and background sites in Europe. Atmos. Environ. 38, 2561–2577. https://doi.org/10.1016/j.atmosenv.2004.01.040.

Van Drooge, B.L., Garatachea, R., Reche, C., Titos, G., Alastuey, A., Lyamani, H., Alados-Arboledas, L., Querol, X., Grimalt, J.O., 2022. Primary and secondary organic winter aerosols in Mediterranean cities under different mixing layer conditions (Barcelona and Granada). Environ. Sci. Pollut. Res. 29, 36255–36272. https://doi.org/10.1007/s11356-021-16366-0.

Vanderstraeten, P., Forton, M., Brasseur, O., Offer, Z.Y., 2011. Black Carbon Instead of Particle Mass Concentration as an Indicator for the Traffic Related Particles in the Brussels Capital Region. J. Environ. Prot. (Irvine Calif). 02, 525–532. https://doi.org/10.4236/jep.2011.25060.

Veld, M. in t., Alastuey, A., Pandolfi, M., Amato, F., Pérez, N., Reche, C., Via, M., Minguillón, M.C., Escudero, M., Querol, X., 2021. Compositional changes of PM2.5 in NE Spain during 2009–2018: A trend analysis of the chemical composition and source apportionment. Sci. Total Environ. 795. doi:10.1016/j.scitotenv.2021.148728.

Vetter, S.G., Ruf, T., Bieber, C., Arnold, W., 2015. What is a mild winter? Regional differences in within-species responses to climate change. PLoS One 10, 1–17. https://doi.org/10.1371/journal.pone.0132178.

Via, M., Minguillón, M.C., Reche, C., Querol, X., Alastuey, A., 2021. Increase in secondary organic aerosol in an urban environment. Atmos. Chem. Phys. 21, 8323–8339. https://doi.org/10.5194/acp-21-8323-2021.

Virkkula, A., 2021. Modeled source apportionment of black carbon particles coated with a light-scattering shell. Atmos. Meas. Tech. 14, 3707–3719. https://doi.org/10.5194/amt-14-3707-2021.

Virkkula, A., Mäkelä, T., Hillamo, R., Yli-Tuomi, T., Hirsikko, A., Hämeri, K., Koponen, I. K., 2007. A simple procedure for correcting loading effects of aethalometer data. J. Air Waste Manag. Assoc. 57, 1214–1222. https://doi.org/10.3155/1047-3289.57.10.1214.

Wang, Q., Liu, H., Ye, J., Tian, J., Zhang, T., Zhang, Y., Liu, S., Cao, J., 2021. Estimating Absorption Ångström Exponent of Black Carbon Aerosol by Coupling Multiwavelength Absorption with Chemical Composition. Environ. Sci. Technol. Lett. 8, 121–127. https://doi.org/10.1021/acs.estlett.0c00829.

Wang, R., Tao, S., Shen, H., Huang, Y., Chen, H., Balkanski, Y., Boucher, O., Ciais, P., Shen, G., Li, W., Zhang, Y., Chen, Y., Lin, N., Su, S., Li, B., Liu, J., Liu, W., 2014. Trend in global black carbon emissions from 1960 to 2007. Environ. Sci. Technol. 48, 6780–6787. https://doi.org/10.1021/es5021422.

Weingartner, E., Saathoff, H., Schnaiter, M., Streit, N., Bitnar, B., Baltensperger, U., 2003. Absorption of light by soot particles: Determination of the absorption coefficient by means of aethalometers. J. Aerosol Sci. 34, 1445–1463. https://doi.org/10.1016/S0021-8502(03)00359-8.

Wen, W., Ma, X., Guo, C., Wei, P., Zhao, X., Xu, J., 2020. Source apportionment of black carbon and the feedback effect on the meteorological factors in Beijing China. Environ. Sci. Pollut. Res.. 41764–41775.

WHO, World Health Organization. Health effects of black carbon. Janssen, Nicole AH, Gerlofs-Nijland, Miriam E, Lanki, Timo, Salonen, Raimo O, Cassee, Flemming. et al. (2012). Health effects of black carbon. World Health Organization. Regional Office for Europe. https://apps.who.int/iris/handle/10665/352615.

WHO, World Health Organization. (2021). WHO global air quality guidelines: particulate matter (PM2.5 and PM10), ozone, nitrogen dioxide, sulfur dioxide and carbon monoxide. World Health Organization. https://apps.who.int/iris/handle/10665/345329. Licencia: CC BY-NC-SA 3.0 IGO.

WMO/GAW Report No. 227, 2016. WMO/GAW Aerosol Measurement Procedures, Guidelines and Recommendations. https://library.wmo.int/ (accessed 8.31.22).

Wood, S.N., 2001. Minimizing model fitting objectives that contain spurious local minima by bootstrap restarting. Biometrics 57, 240–244. https://doi.org/10.1111/j.0006-341X.2001.00240.x.

Wu, B., Xuan, K., Zhang, X., Shen, X., Li, X., Zhou, Q., Cao, X., Zhang, H., Yao, Z., 2021. Mass absorption cross-section of black carbon from residential biofuel stoves and diesel trucks based on real-world measurements. Sci. Total Environ. 784, 147225 https://doi.org/10.1016/j.scitotenv.2021.147225.

Yttri, K.E., Simpson, D., Nojgaard, J.K., Kristensen, K., Genberg, J., Stenström, K., Swietlicki, E., Hillamo, R., Aurela, M., Bauer, H., Offenberg, J.H., Jaoui, M., Dye, C., Eckhardt, S., Burkhart, J.F., Stohl, A., Glasius, M., 2011. Source apportionment of

the summer time carbonaceous aerosol at Nordic rural background sites. Atmos. Chem. Phys. 11, 13339–13357. https://doi.org/10.5194/acp-11-13339-2011.

Yuan, J., Lewis Modini, R., Zanatta, M., Herber, A.B., Müller, T., Wehner, B., Poulain, L., Tuch, T., Baltensperger, U., Gysel-Beer, M., 2021. Variability in the mass absorption cross section of black carbon (BC) aerosols is driven by BC internal mixing state at a central European background site (Melpitz, Germany) in winter. Atmos. Chem. Phys. 21, 635–655. https://doi.org/10.5194/acp-21-635-2021.

Yus-Díez, J., Bernardoni, V., Močnik, G., Alastuey, A., Ciniglia, D., Ivančič, M., Querol, X., Perez, N., Reche, C., Rigler, M., Vecchi, R., Valentini, S., Pandolfi, M., 2021. Determination of the multiple-scattering correction factor and its cross-sensitivity to scattering and wavelength dependence for different AE33 Aethalometer filter tapes: a multi-instrumental approach. Atmos. Meas. Tech. Discuss. 14, 6335–6355. https://doi.org/10.5194/amt-2021-46.

Zanatta, M., Gysel, M., Bukowiecki, N., Müller, T., Weingartner, E., Areskoug, H., Fiebig, M., Yttri, K.E., Mihalopoulos, N., Kouvarakis, G., Beddows, D., Harrison, R. M., Cavalli, F., Putaud, J.P., Spindler, G., Wiedensohler, A., Alastuey, A., Pandolfi, M., Sellegri, K., Swietlicki, E., Jaffrezo, J.L., Baltensperger, U., Laj, P., 2016. A European aerosol phenomenology-5: Climatology of black carbon optical properties at 9 regional background sites across Europe. Atmos. Environ. 145, 346–364. https://doi.org/10.1016/j.atmosenv.2016.09.035.

Zhang, Y., Albinet, A., Petit, J.E., Jacob, V., Chevrier, F., Gille, G., Pontet, S., Chrétien, E., Dominik-Sègue, M., Levigoureux, G., Močnik, G., Gros, V., Jaffrezo, J.L., Favez, O., 2020c. Substantial brown carbon emissions from wintertime residential wood burning over France. Sci. Total Environ. 743 https://doi.org/10.1016/j.scitotenv.2020.140752.

Zhang, Y., Favez, O., Canonaco, F., Liu, D., Prévôt, A.S.H., Gros, V., Albinet, A., 2018. Evidence of major secondary organic aerosol contribution to lensing effect black carbon absorption enhancement. doi:10.1038/s41612-018-0056-2.

Zhang, X., Mao, M., Chen, H., Tang, S., 2020a. The Angstrom exponents of black carbon aerosols with non-absorptive coating: A numerical investigation. J. Quant. Spectrosc. Radiat. Transf. 257, 107362 https://doi.org/10.1016/j.jqsrt.2020.107362.

Zhang, X., Mao, M., Yin, Y., Tang, S., 2020b. The absorption Ångstrom exponent of black carbon with brown coatings: Effects of aerosol microphysics and parameterization. Atmos. Chem. Phys. 20, 9701–9711. https://doi.org/10.5194/acp-20-9701-2020.

Zhang, G., Peng, L., Lian, X., Lin, Q., Bi, X., Chen, D., Li, M., Li, L., Wang, X., Sheng, G., 2019a. An improved absorption Ångström exponent (AAE)-based method for evaluating the contribution of light absorption from brown carbon with a high-time resolution. Aerosol Air Qual. Res. 19, 15–24. https://doi.org/10.4209/aaqr.2017.12.0566.

Zhang, Q., Wan, Z., Hemmings, B., Abbasov, F., 2019b. Reducing black carbon emissions from Arctic shipping: Solutions and policy implications. J. Clean. Prod. 241, 118261 https://doi.org/10.1016/j.jclepro.2019.118261.

Zhao, W., Tan, W., Zhao, G., Shen, C., Yu, Y., Zhao, C., 2021. Determination of equivalent black carbon mass concentration from aerosol light absorption using variable mass absorption cross section. Atmos. Meas. Tech. 14, 1319–1331. https://doi.org/10.5194/amt-14-1319-2021.

Zioła, N., Błaszczak, B., Klejnowski, K., 2021. Long-term ebc measurements with the use of maap in the polluted urban atmosphere (Poland). Atmosphere (Basel). 12, 1–23. https://doi.org/10.3390/atmos12070808.

Zotter, P., Herich, H., Gysel, M., El-Haddad, I., Zhang, Y., Mocnik, G., Hüglin, C., Baltensperger, U., Szidat, S., Prévôt, A.S.H., 2017. Evaluation of the absorption Ångström exponents for traffic and wood burning in the Aethalometer-based source apportionment using radiocarbon measurements of ambient aerosol. Atmos. Chem. Phys. 17, 4229–4249. https://doi.org/10.5194/acp-17-4229-2017.